Geochemical and Sr-Nd Isotopic Characteristics of Post-Collisional Calc-Alkaline Volcanics in the Eastern Pontides (NE Turkey)

ABDULLAH KAYGUSUZ

MEHMET ARSLAN

WOLFGANG SIEBEL

CÜNEYT ŞEN

Geochemical and Sr-Nd Isotopic Characteristics of Post-Collisional Calc-Alkaline Volcanics in the Eastern Pontides (NE Turkey)

ABDULLAH KAYGUSUZ[1], MEHMET ARSLAN[2], WOLFGANG SIEBEL[3] & CÜNEYT ŞEN[2]

[1] Department of Geological Engineering, Gümüşhane University, TR–29000 Gümüşhane,
Turkey (E-mail: abdullah.kaygusuz@gmail.com)

[2] Department of Geological Engineering, Karadeniz Technical University, TR–61080 Trabzon, Turkey

[3] Institute of Geosciences, Universität Tübingen, Wilhelmstr. 56, D-72074 Tübingen, Germany

Abstract: Major, trace element, K-Ar age and Sr-Nd isotopic data are presented for the Eocene Torul volcanics in the eastern Pontide orogenic belt (NE Turkey). The studied rocks are composed of basaltic andesitic, andesitic, trachyandesitic, and minor trachydacitic lavas associated with their pyroclastics. These rocks contain plagioclase (An_{2-44}), hornblende (Mg#= 0.78–0.98), clinopyroxene ($Wo_{43-46} En_{41-43} Fs_{10-15}$), biotite, quartz, and minor sanidine phenocrysts. K-Ar ages on hornblendes ages range from 43.99 (±2.59) to 33.45 (±2.32) Ma, within the Middle to Late Eocene. The volcanic rocks show calc-alkaline affinities and have medium to high K contents. They are enriched in large ion lithophile (LILE) and light rare earth elements (LREE), with pronounced depletion of high field strength elements (HFSE). The chondrite-normalized REE patterns (La_{cn}/Lu_{cn}= 4.0–9.8) show low to medium enrichment, indicating similar sources for the rock suite. Initial $^{87}Sr/^{86}Sr$ values vary between 0.70457 and 0.70511 and initial $^{143}Nd/^{144}Nd$ values between 0.51264 and 0.51278. The main solidification processes involved in the evolution of the volcanics consist of fractional crystallization with minor amounts of crustal contamination ± magma mixing. All evidence supports the conclusion that the parental magma(s) of the rocks probably derived from an enriched upper mantle, previously modified by subduction- induced metasomatism in a post-collisional geodynamic setting.

Key Words: eastern Pontides, geochemistry, Sr-Nd isotopes, post-collisional magmatism, Torul volcanics

Doğu Pontidlerde (KD Türkiye) Çarpışma Sonrası Kalk-Alkalen Volkanizmanın Jeokimyası ve Sr-Nd İzotopik Karakterleri

Özet: Doğu Pontidlerde Eosen yaşlı Torul volkanitlerinin ana, iz element, K-Ar yaş ve Sr-Nd izotop verileri incelenmiştir. İncelenen volkanitler, bazaltik andezit, andezit, trakiandezit ve az oranda da trakidasit ve bunların piroklastiklerinden oluşurlar. Volkanitler plajiyoklas (An_{2-44}), hornblend (Mg#= 0.78–0.98), klinopiroksen ($Wo_{43-46} En_{41-43} Fs_{10-15}$), biyotit, kuvars ve az oranda da sanidin fenokristallerinden oluşurlar. Hornblendlerdeki K-Ar yaşları, 43.99 (±2.59) – 33.45 (±2.32) My aralığında olup, Torul volkanitlerinin Orta–Geç Eosen zamanında oluştuklarını göstermektedir. Torul volkanitleri kalk-alkalen karakterli olup orta–yüksek K içeriğine sahiptirler. Volkanitler büyük iyon yarıçaplı elementler (LILE) ve hafif hafif nadir toprak elementlerce (LREE) zenginleşmiş, yüksek çekim alanlı elementlerce (HFSE) tüketilmişlerdir. Kondrite normalize edilmiş nadir toprak element dağılımları, düşük–orta derecede zenginleşmeyle konkav şekilli olup (La_{cn}/Lu_{cn}= 4.0–9.8), volkanitleri oluşturan kayaçların benzer kaynaktan itibaren oluştuklarını düşündürmektedir. $^{87}Sr/^{86}Sr_{(i)}$ değerleri 0.70457–0.70511 arasında olup $^{143}Nd/^{144}Nd_{(i)}$ değerleri 0.70457–0.70511 arasındadır. Volkanitlerin gelişiminde başlıca fraksiyonel kristallenme, daha az oranda da kabuksal kirlenme ± magma karışımı rol oynamıştır. Tüm bu veriler, volkanitlerin köken magma(lar)sının muhtemelen daha önceki yitim akışkanları tarafından metasomatizmaya uğratılmış zenginleşmiş bir üst manto kaynağından, çarpışma sonrası jeodinamik bir ortamda türeyebileceklerini ifade etmektedir.

Anahtar Sözcükler: doğu Pontidler, jeokimya, Sr-Nd izotop, çarpışma sonrası magmatizma, Torul volkanitleri

Introduction

The eastern Pontides are an example of long-term crustal evolution from pre-subduction rifting, through island arc volcanism and plutonism to post-subduction alkaline volcanism (e.g., Akın 1978; Şengör & Yılmaz 1981; Akıncı 1984). The eastern Pontides are characterized by three volcanic cycles developed during Liassic, Late Cretaceous and Eocene times (Çamur *et al.* 1996; Arslan *et al.* 1997). Although many authors have addressed the evolution of the volcanic rocks in the eastern Pontides (e.g., Adamia *et al.* 1977; Tokel 1977; Kazmin *et al.* 1986; Çamur *et al.* 1996; Arslan *et al.* 1997, 2000a & b, 2002, 2007a & b, 2009; Şen *et al.* 1998; Arslan & Aliyazıcıoğlu 2001; Temizel & Arslan 2003, 2005, 2008, 2009; Şen 2007; Altherr *et al.* 2008; Aydın *et al.* 2008), isotopic and petrogenetic studies are limited in the region. Tokel (1977) noted the calc-alkaline composition of the volcanic rocks, reflecting features of island-arc volcanism. Çamur *et al.* (1996) and Arslan *et al.* (1997) suggested that the volcanic rocks were derived from an enriched MORB-like mantle source, and are related to subduction processes. Arslan *et al.* (1997) reported that the general geochemical characteristics of the volcanics imply that their parental magma was derived from the upper mantle and/or lower crust. Geochemical data show that the volcanic rocks are mainly calc-alkaline, with moderate potassium enrichment. They evolved by shallow-level fractional crystallization, magma mixing and contamination of a parental magma. Aydın *et al.* (2008) suggested that enriched subcontinental lithospheric mantle played a role during the formation of the Neogene alkaline volcanic rocks in the Trabzon area. Arslan *et al.* (2007a, b, 2009) reported that the variety and distribution of volcanic rocks, together with petrological data, indicate that Tertiary volcanic activity in the eastern Pontides is closely related to the thinning of young lithosphere caused by a transtensional tectonic regime developed by Late Cretaceous–Eocene slab break-off in the Pontide palaeo-magmatic arc. Moreover, the calc-alkaline nature of the Eocene volcanism may be connected with an increasingly geodynamic regime and compression following the slab break off (Arslan *et al.* 2007a, b, 2009).

Apart from some recent age and isotopic data obtained from Eocene volcanic rocks in the southernmost part of the eastern Pontide belt (Arslan *et al.* 2007a; Temizel 2008), such data are lacking from other parts of the volcanic belt, including the Torul area. In this study, new petrographic, geochemical and Sr-Nd isotopic data for volcanic rocks in the Torul (Gümüşhane) area are reported that contribute to the formation and magmatic evolution of the widespread eastern Pontide Eocene volcanism.

Regional Geology and Stratigraphy

Based on structural and lithological differences the eastern Pontide belt is commonly subdivided into a northern and southern zone (Figure 1) (Özsayar *et al.* 1981; Okay & Şahintürk 1997). Upper Cretaceous and Middle Eocene volcanic and volcaniclastic rocks dominate the northern zone, whereas pre-Late Cretaceous rocks are widely exposed in the southern zone (Arslan *et al.* 1997, 2000a, 2002; Şen *et al.* 1998; Şen 2007). The volcanic rocks of the eastern Pontides lie unconformably on a Palaeozoic heterogeneous crystalline basement, and are intruded by granitoids (Yılmaz 1972; Çoğulu 1975; Okay & Şahintürk 1997; Topuz *et al.* 2001; Topuz 2002). Volcanic and volcano-sedimentary rocks of Jurassic age lie unconformably on the basement. These rocks are tholeiitic in character and mostly crop out in the southern zone. They consist of basaltic, minor andesitic and trachyandesitic lavas and pyroclastic equivalents. The Jurassic volcanics are overlain conformably by Jurassic–Cretaceous neritic and pelagic carbonates. The Upper Cretaceous series that unconformably overlies these carbonate rocks consists of sedimentary rocks in the southern part, and of volcanic rocks in the northern parts (Bektaş *et al.* 1987; Robinson *et al.* 1995; Yılmaz & Korkmaz 1999). The Cretaceous volcanic rocks are tholeiitic to calc-alkaline in composition and comprise dacites, rhyolites and minor andesites, basalts, and their pyroclastic equivalents. Plutonic rocks (Figure 1) were also emplaced between Jurassic and Palaeocene time (Okay & Şahintürk 1997; Yılmaz *et al.* 1997; Kaygusuz *et al.* 2008, 2009; Kaygusuz & Aydınçakır 2009).
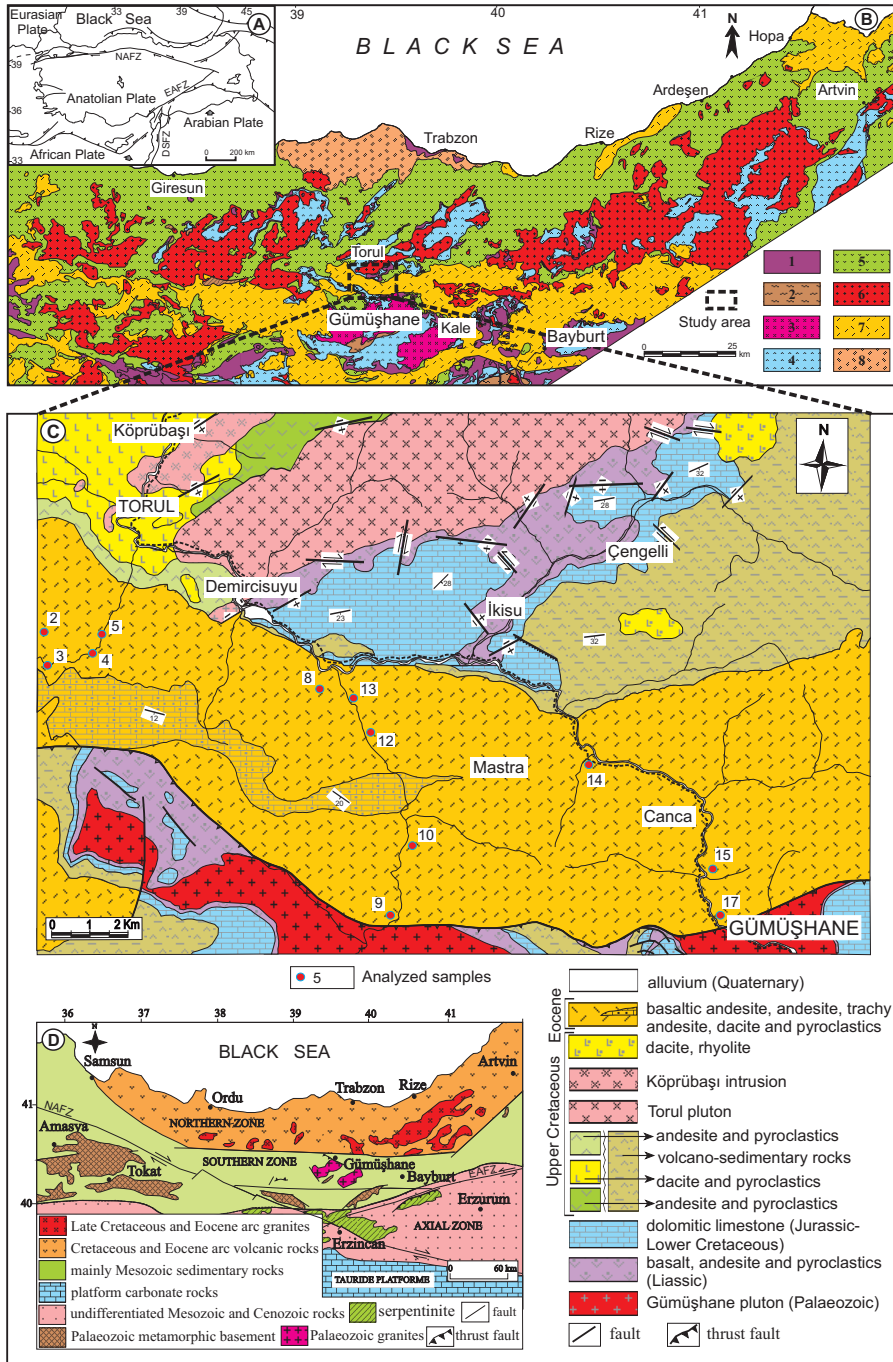
Figure 1. (a) Tectonic map of Turkey and surroundings (modified after Şengör *et al.* 2003); (b) distribution of volcanic units in the eastern Pontides (modified from Güven 1993); (c) geological map of the study area (modified after Jica 1986 and Kaygusuz 2000), and (d) major structures of the eastern Pontides (modified from Eyüboğlu *et al.* 2007). 1– Permo–Carbonifeous terrigenes, 2– Palaeozoic metamorphic rocks, 3– Palaeozoic granitoids, 4– Jurassic–Lower Cretaceous volcanic rocks, 5– Upper Cretaceous volcanic rocks, 6– Upper Cretaceous–Eocene granitoids, 7– Tertiary calc-alkaline volcanic rocks, 8– Tertiary alkaline volcanic rocks. NAFZ– North Anatolian Fault Zone, EAFZ– East Anatolian Fault Zone.

The Eocene volcanic rocks uncoformably overlie the Upper Cretaceous series (Güven 1993; Yılmaz & Kokmaz 1999). During Palaeocene–Early Eocene time, the eastern Pontides were above sea level, probably due to the collision of the Eurasian and Arabian plates (Okay & Şahintürk 1997; Boztuğ *et al.* 2004). Calc-alkaline to alkaline Tertiary volcanic rocks (Figure 1a) are exposed in the Trabzon and Tonya region (northern zone) and in the Gümüşhane and Ordu region (southern zone) (Arslan *et al.* 1997, 2000a, b, 2001, 2002, 2007a, b; Şen *et al.* 1998; Temizel & Arslan 2003, 2005, 2008, 2009; Aydın 2004; Şen 2007; Temizel 2008; Yücel *et al.* 2009). The Eocene volcanic and volcaniclastic rocks are intruded by calc-alkaline granitoids of similar age (44 Ma; Arslan & Aslan 2006). Post-Eocene uplift and erosion was accompanied by clastic deposition in locally developed basins (Korkmaz *et al.* 1995). From the end of the Middle Eocene, the region remained largely above sea level, with minor volcanism and terrigeneous sedimentation continuing until the present (Okay & Şahintürk 1997). The Miocene and post-Miocene volcanic history of the eastern Pontides is characterized by calc-alkaline to mildly alkaline volcanism (Aydın 2004; Arslan *et al.* 2007a; Temizel 2008).

The Torul area is located at the transition between the northern and southern zones of the eastern Pontides, NE Turkey (Figure 1). This region exposes Liassic, Upper Cretaceous and Tertiary volcanic rocks (Kaygusuz 2000; Kaygusuz *et al.* 2006). Liassic volcanics are tholeiitic to calc-alkaline and consist mainly of basalts, andesites and their pyroclastic equivalents (Kaygusuz 2000; Şen 2007). They are overlain conformably by Jurassic–Cretaceous carbonates. The Late Cretaceous series that unconformably overlies these carbonate rocks is dominated by sedimentary rocks in the southern part, and by volcanic rocks in the northern part of study area. The volcanic rocks are calc-alkaline and consist mainly of andesite, dacite, rhyolite and their pyroclastic equivalents (Kaygusuz 2000; Kaygusuz *et al.* 2006). The sedimentary and volcanoclastic rocks comprise turbiditic flysch consisting of tuff with locally interbedded alternating limestone, marl, sandstone, and siltstone. The Torul (77–80 Ma, Kaygusuz *et al.* 2008) and the Köprübaşı plutons (79 Ma, Kaygusuz & Şen 2010) cut all these lithologies,

and the Tertiary volcanic rocks unconformably overlie all of these rocks. All these units are overlain unconformably by Quaternary alluvium.

In the Torul region, the Eocene sequence consists mainly of basalt, andesite with minor dacite and associated pyroclastics. The unit, which is underlain by upper Cretaceous basement comprising alternating limestone, marl, sandstone, siltstone and tuff, starts with a thin to medium-bedded micritic limestones. These basement units are overlain by a thick volcanic sequence including basalt, andesite, minor dacite and their pyroclastic equivalents. The top of the unit consists of sedimentary rocks, consisting of sandstone, siltstone and marl. Andesitic rocks are the dominant lithology within the seqence. They are characterized by their greenish grey to dark grey colours in the field and the existence of euhedral to subhedral hornblende and plagioclase phenocrysts in hand specimen. Basaltic rocks are also minor constituents of the sequence. Fresh surfaces are characteristically black and dark grey. Dacitic rocks make up volumetrically minor constituents of the sequence. The pyroclastic rocks are mainly represented by basaltic agglomerates, succeeded by medium- to thick-bedded (5–45 cm) tuffs and basaltic/rarely andesitic breccias (10–50 cm in diameter). Rounded agglomerate blocks ranging from 5 to 50 cm in diameter, have been cemented by a fine-grained, altered, greenish-brownish volcanic matrix. Andesitic, basaltic and dacitic tuffs and tuffites, whose bedding thicknesses changes from 15 cm to 80 cm, are volumetrically minor with respect to the other members within the sequence. They exhibit abrupt thickness changes within short distances as in most pyroclastic successions. The total thickness of the Eocene sequence is more than 500 m in the Torul area.

Analytical Techniques

A total of 120 rock samples were collected from the volcanic rocks in the Torul (Gümüşhane) area. Their mineralogical compositions and textures were studied using a binocular polarizing microscope. Based on these studies, 12 of the freshest and most representative rock samples were selected for whole-rock major element, trace element, and REE analysis.

Major and trace elements were determined by ICP-emission spectrometry and ICP-mass spectrometry using standard techniques at ACME, Analytical Laboratories Ltd., Vancouver (Canada). 0.2 g of rock-powder was fused with 1.5 g $LiBO_2$ and dissolved in 100 ml 5% HNO_3. Loss on ignition (LOI) was determined on the dried samples heated to a temperature of 1000 °C. REE analyses were performed by ICP-MS at ACME. Detection limits ranged from 0.01 to 0.1 wt % for major oxides, from 0.1 to 10 ppm for trace elements, and from 0.01 to 0.5 ppm for REE.

Mineral analyses were conducted in the Electron Microprobe Laboratory at the University of New Brunswick (Canada). Measurements were made on a JEOL JSM-6400 scanning electron microscope, equipped with a Link eXL energy-dispersive analyser and a single-wavelength dispersive channel. Analyses were carried out at an acceleration potential of 15 kV under sample currents of 2.5 nA, using 100 s for energy-dispersive data acquisition. Data were reduced with the Link ZAF procedure using a combination of mineral (orthoclase-K, albite-Na, hornblende-Al, olivine-Mg, pyroxene-Si, K, Ca and metals such as Fe and Ti) standards. The analytical results are presented in Tables 1–4. Detection limits are generally about 0.1 wt%.

Hornblende separates (200–300 μm) were obtained using conventional heavy liquid and magnetic separation procedures in the mineral-separation laboratories of the Institute of Geology and Geophysics, Chinese Academy of Sciences (Beijing). K-Ar isotopic analyses of these samples were performed at the Institute of Geology and Geophysics, Chinese Academy of Sciences (Beijing). Potassium contents were analyzed using a spectrophotometer (type 6400) and two standards (biotite ZBH-25, trachyte ZGC) for callibration. The argon contents were measured using a RGA10 mass-spectrometer, and were adjusted to a biotite standard ZBH-25 and a trachyte standard ZGC. The parameters used in the age calculation were: $\lambda = 5.543 \times 10^{-10}$/year, $^{40}K/\Sigma K = 1.167 \times 10^{-4}$.

Nd and Sr isotope analyses were conducted at the Institute of Geology and Geophysics, Chinese Academy of Sciences, Beijing. Samples were dissolved using acid (HF + $HClO_4$) in sealed Savillex

beakers on a hot plate for one week. Separation of Rb, Sr and light REE was achieved through a cation-exchange column (packed with BioRad AG 50W-X8 resin). Sm and Nd were further purified using a second cation-exchange column that was conditioned and eluted with diluted HCl. Mass analyses were conducted using a multicollector VG354 mass spectrometer as described by Qiao (1988). $^{87}Sr/^{86}Sr$ and $^{143}Nd/^{144}Nd$ ratios were corrected for mass fractionation relative to $^{86}Sr/^{88}Sr = 0.1194$ and $^{146}Nd/^{144}Nd = 0.7219$, respectively. Finally, the $^{87}Sr/^{86}Sr$ ratios were adjusted to the NBS-987 Sr standard = 0.710250, and the $^{143}Nd/^{144}Nd$ ratios to the La Jolla Nd standard = 0.511860. The uncertainty in concentration analyses by isotopic dilution is 2% for Rb, 0.5% for Sr, and 0.2–0.5% for Sm and Nd, depending upon concentration levels. Procedural blanks are: Rb= 80 pg, Sr= 300 pg, Sm= 50 pg and Nd= 50–100 pg. The detailed explanation of sample preparation, errors and analytical precision is provided in Zhang *et al.* (2002).

Petrography and Mineral Chemistry

Based on their mineralogical, petrographic, and textural characteristics, the volcanic rocks of the Torul area are mainly basaltic andesites, andesites, trachyandesites, and minor trachydacites. Basaltic andesites have microlitic to microlitic-porphyric textures with plagioclase, clinopyroxene and hornblende phenocrysts. Their groundmass has an intergranular texture and contains plagioclase, clinopyroxene, hornblende, Fe-Ti oxide, and volcanic glass (Figure 2a). Andesites exhibit hypocrystalline porphyritic and glomeroporphyritic textures with phenocrysts of plagioclase, hornblende and clinopyroxene (Figure 2b). Their groundmass has a hyalopilitic texture and includes plagioclase microlites, hornblende, clinopyroxene, Fe-Ti oxide, and volcanic glass. Trachyandesites have microlitic-porphyric textures with plagioclase, K-feldspar (less than 10% of the total feldspars), hornblende and clinopyroxene phenocrysts. Their groundmass has an intergranular and trachytic texture and contains plagioclase, hornblende, clinopyroxene, Fe-Ti oxide, and volcanic glass. Dacites display holocrystalline- and microgranular textures characterized by plagioclase, quartz, hornblende and biotite
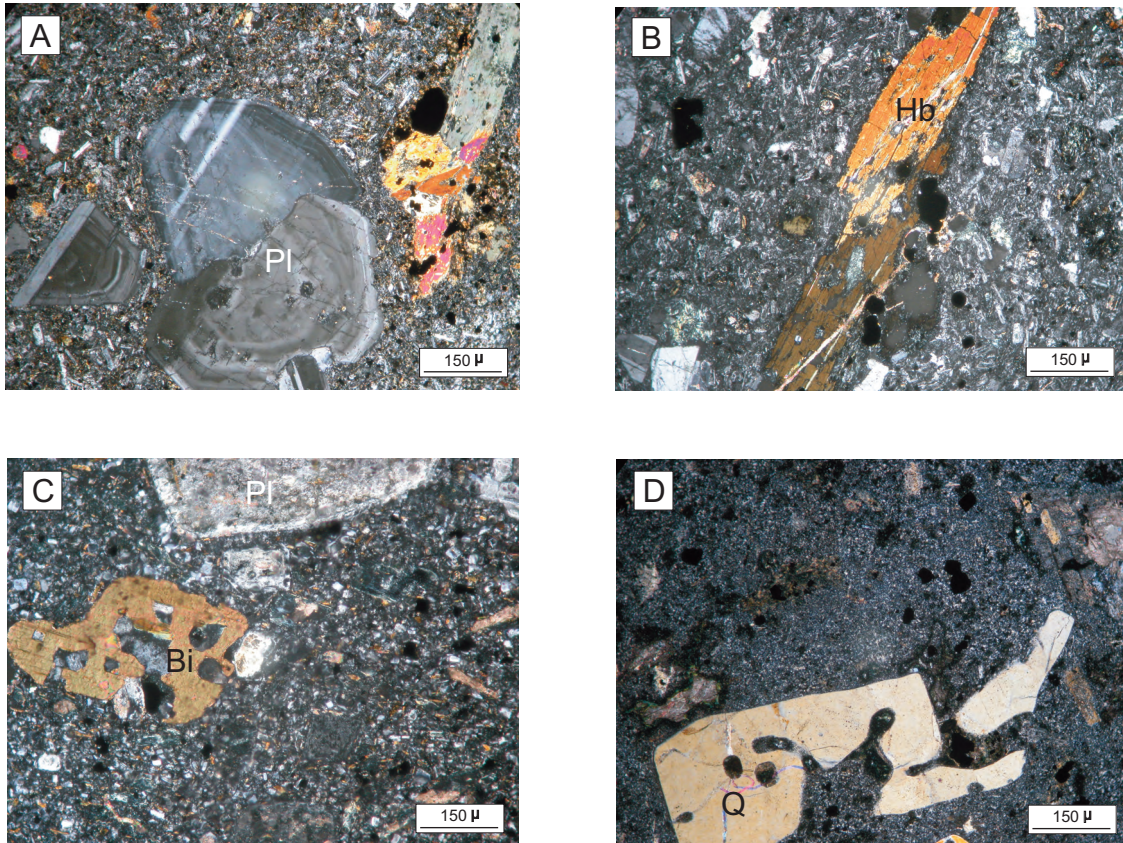
Figure 2. Microphotographs showing textural features of the Torul volcanic rocks: **(a)** oscillatory zoning; **(b, c)** poikilitic textures in hornblende and biotite in which some large hornblende and biotite may contain small plagioclase and opaque minerals; **(d)** embayed quartz crystals. Pl– plagioclase, Hbl– hornblende, Bi– biotite, Q– quartz.

phenocrysts set in a groundmass of microlites of plagioclase, hornblende, biotite, Fe-Ti oxide, and glass (Figure 2c, d).

Plagioclase is the most common phenocryst phase and occurs in all rock types. It mainly forms euhedral to subhedral, normal and reverse zoned microlites and phenocrysts (up to 2.5 mm). Crystals show oscillatory zoning (Figure 2a) and prismatic-cellular growth. Some samples have poikilitic textures, in which large plagioclase crystals (up to 2 mm) may contain small crystals of plagioclase and opaque minerals. A wide range in anorthite composition (Table 1) can be found, ranging from An_{29} to An_{43} in basaltic andesites and from An_2 to An_{28} in andesites. Sanidine is found in trachyandesitic rocks as subhedral to anhedral

microphenocrysts. Hornblende occurs as euhedral to subhedral phenocrysts and microlites in groundmasses. Phenocrysts (up to 2 mm) are common in all rock types. Hornblende displays a narrow compositional range and is classified as Mg-hastingsite and Mg-hastingsitic hornblende (Mg# = 0.78–0.98) (Table 1; Leake *et al.* 1997). The Mg-number [(Mg#= atomic ratios Mg/(Mg+Fe), where Fe is total iron)] ranges from 0.82 to 0.98 in basaltic andesites and from 0.78 to 0.87 in andesites (Table 1). Larger crystals may contain small plagioclase and opaque minerals (Figure 2b). Pyroxene forms euhedral to subhedral crystals, and occurs in glomeroporphyritic aggregates together with plagioclase and Fe-Ti oxides. Pyroxene phenocrysts (up to 2 mm) are common in basaltic andesites.

Table 1. Microprobe analyses of plagioclase, hornblende and pyroxene from the Torul volcanic rocks.

Plagioclase

Rock Types	Basaltic andesite						Andesite			
Samples	12-1	12-2	12-3	9-1	9-2	avg (n=5)	13-2	5-1	5-2	avg (n=3)
SiO_2	64.27	52.90	52.78	62.46	62.97	59.08	66.33	67.30	64.43	66.02
TiO_2	0.00	0.00	0.00	0.00	0.00	0.00	0.00	0.00	0.00	0.00
Al_2O_3	20.60	25.09	24.43	20.93	21.05	22.42	22.39	21.11	21.14	21.55
FeO^T	0.00	0.29	0.31	0.00	0.03	0.13	0.00	0.10	0.02	0.04
MgO	0.00	0.00	0.00	0.00	0.00	0.00	0.00	0.00	0.00	0.00
CaO	6.05	6.44	6.49	7.29	6.34	6.52	1.77	0.43	6.36	2.85
Na_2O	8.22	4.62	4.48	9.84	10.09	7.45	11.11	11.71	9.20	10.67
K_2O	0.01	0.12	0.12	0.01	0.00	0.05	0.00	0.07	0.01	0.03
Sum	100.2	101.5	101.6	100.5	101.5	101.0	101.6	100.7	102.2	101.5
Si	8.24	7.52	7.57	8.01	8.06	7.88	8.25	8.42	8.14	8.27
Ti	0.00	0.00	0.00	0.00	0.00	0.00	0.00	0.00	0.00	0.00
Al	3.11	4.20	4.13	3.16	3.17	3.56	3.28	3.11	3.15	3.18
Fe^{2+}	0.00	0.03	0.04	0.00	0.00	0.01	0.00	0.01	0.00	0.00
Mg	0.00	0.00	0.00	0.00	0.00	0.00	0.00	0.00	0.00	0.00
Ca	0.83	0.98	1.00	1.00	0.87	0.94	0.24	0.06	0.86	0.38
Na	2.04	1.27	1.25	2.45	2.50	1.90	2.68	2.84	2.25	2.59
K	0.00	0.02	0.02	0.00	0.00	0.01	0.00	0.01	0.00	0.00
Sum ct.	14.23	14.03	14.00	14.63	14.61	14.30	14.45	14.45	14.41	14.44
Ca+Na+K	2.88	2.28	2.26	3.45	3.37	2.85	2.92	2.91	3.12	2.98
An	28.90	43.10	44.03	29.03	25.77	34.17	8.09	1.98	27.63	12.57
Ab	71.05	55.95	55.00	70.92	74.23	65.43	91.91	97.63	72.32	87.29
Or	0.06	0.96	0.97	0.05	0.00	0.41	0.00	0.38	0.05	0.15

structural formula on the basis of 32 oxygen atoms

Hornblende

Rock Types	Basaltic andesite					Andesite		
Samples	9-1	9-2	12-1	12-2	avg (n=4)	5-1	5-2	avg (n=2)
SiO_2	43.12	43.52	43.05	42.51	43.05	44.92	44.57	44.75
TiO_2	1.32	1.28	1.27	1.06	1.23	1.05	1.09	1.07
Al_2O_3	12.14	13.23	12.32	14.14	12.96	10.78	11.19	10.99
Cr_2O_3	0.00	0.02	0.00	0.04	0.02	0.07	0.09	0.08
FeO	9.98	9.31	14.95	11.67	11.48	13.73	15.14	14.44
MnO	0.10	0.10	0.51	0.16	0.22	0.39	0.54	0.47
MgO	15.67	16.51	12.72	14.76	14.92	14.09	12.74	13.42
CaO	11.06	11.90	11.14	11.64	11.44	11.26	11.22	11.24
Na_2O	2.15	2.36	1.96	2.35	2.21	1.71	1.76	1.74
K_2O	0.45	0.47	0.48	0.44	0.46	0.39	0.52	0.46
Sum	96.0	98.7	98.4	98.8	98.0	98.4	98.9	98.6
Si	6.21	6.11	6.19	6.02	6.13	6.40	6.39	6.39
Ti	0.14	0.14	0.14	0.11	0.13	0.11	0.12	0.12
Al^{4+}	1.79	1.89	1.81	1.98	1.87	1.60	1.61	1.61
Al^{6+}	0.28	0.30	0.28	0.37	0.31	0.21	0.28	0.25
Cr	0.00	0.00	0.00	0.00	0.00	0.00	0.00	0.00
Fe^{2+}	0.08	0.09	0.60	0.25	0.25	0.45	0.75	0.60
Fe^{3+}	1.13	1.01	1.19	1.13	1.11	1.18	1.07	1.12
Mn	0.01	0.01	0.06	0.02	0.03	0.05	0.07	0.06
Mg	3.37	3.46	2.73	3.11	3.17	2.99	2.72	2.86
Ca	1.71	1.79	1.72	1.76	1.74	1.72	1.72	1.72
Na	0.60	0.64	0.55	0.64	0.61	0.47	0.49	0.48
K	0.08	0.08	0.09	0.08	0.08	0.07	0.10	0.08
Sum ct.	15.39	15.52	15.35	15.49	15.44	15.26	15.31	15.28
Mg#	0.98	0.98	0.82	0.93	0.92	0.87	0.78	0.83
P (kbar)[a]	6.45	7.10	6.58	7.94	7.02	5.19	5.59	5.39
P (kbar)[b]	6.87	7.59	7.01	8.54	7.50	5.45	5.90	5.68
P (kbar)[c]	6.80	7.41	6.93	8.21	7.34	5.61	5.99	5.80
T (°C)[d]	915.3	943.8	933.0	944.6	934.2	903.5	900.4	902.0

Structural formula on the basis of 23 oxygen atoms

Pyroxene

Rock Types	Basaltic andesite			
Samples	12-1	12-2	9-1	avg (n=3)
SiO_2	50.38	52.16	50.26	50.93
TiO_2	0.58	0.52	0.59	0.56
Al_2O_3	3.86	1.41	4.60	3.29
Cr_2O_3	0.16	0.11	0.33	0.20
FeO	9.03	7.81	6.34	7.73
MnO	0.28	0.46	0.14	0.29
MgO	14.52	15.81	15.48	15.27
CaO	21.16	21.78	22.79	21.91
Na_2O	0.38	0.40	0.24	0.34
K_2O	0.00	0.03	0.00	0.01
Sum	100.4	100.5	100.8	100.5
Si	1.88	1.93	1.85	1.89
Ti	0.02	0.01	0.02	0.02
Al^{4+}	0.12	0.06	0.15	0.11
Al^{6+}	0.05	0.00	0.05	0.03
Cr	0.00	0.00	0.01	0.01
Fe^{2+}	0.18	0.13	0.08	0.13
Fe^{3+}	0.10	0.11	0.11	0.11
Mn	0.01	0.01	0.00	0.01
Mg	0.81	0.87	0.85	0.84
Ca	0.84	0.86	0.90	0.87
Na	0.03	0.03	0.02	0.02
K	0.00	0.00	0.00	0.00
Sum ct.	4.03	4.03	4.04	4.03
Wo	42.95	42.78	45.78	43.84
En	41.02	43.21	43.28	42.50
Fs	14.63	12.58	10.07	12.43
Mg#	0.82	0.87	0.92	0.87

Structural formula on the basis of 6 oxygen atoms

FeO^T is total iron as FeO, $Mg\#$ (mg-number)= $100 \times MgO/(MgO+ FeO^T)$, Sum ct– total cations, avg– average. [a] Hammastrom & Zen (1986), [b] Hollister *et al.* (1987) and [c] Schmidt (1992) formulations used to calculate pressures from hornblendes. [d] Blundy & Holland (1990) formulation used to calculate temperatures from hornblende-plagioclase pairs.

Some minerals are uralitized or replaced by calcite. Using the classification of Morimoto (1988), pyroxene is augite and minor diopside (Wo_{43-46} En_{41-43} Fs_{10-15}) in composition. The Mg-number of the pyroxenes varies between 0.82 and 0.92 (Table 1). Biotite and quartz are found in dacitic rocks as euhedral to subhedral crystals. Some biotites phenocrysts may contain small plagioclase and opaque minerals (Figure 2c). Embayed quartz crystals are common (Figure 2d).

Crystallization conditions of the Torul volcanic rocks were calculated from minerals and/or mineral pairs. Based on Al-in-hornblende barometry (Hammastrom & Zen 1986; Anderson & Smith 1995; Hollister *et al.* 1987) and plagioclase-hornblende thermometry (Blundy & Holland 1990), the minerals crystallized at 900–945 °C under 5.2–8.5 kbar pressures (Table 1).

K-Ar Age Dating

The K-Ar age determinations on the hornblende separates of three volcanic samples are presented in Table 2. The hornblendes samples yield ages of 44.0±2.6 Ma for the basaltic andesitic lava flow, 40.4±2.5 Ma for the andesitic lava flow and 33.5±2.3 Ma for the trachydacitic lava flow, corresponding to the middle to late Eocene.

Whole-Rock Geochemistry

Major and trace element analyses, including REE, of the representative whole rock samples from the Torul volcanic rocks are given in Tables 3 & 4. All rocks display a narrow compositional range with SiO_2 contents ranging from 54 to 64 wt% (Table 3). Mg-numbers range from 24 to 43. The MgO and $Fe_2O_3^T$

contents range from 1.6% to 4.5% and from 4.8% to 8.1%, respectively. In the total alkali-silica diagram (TAS), the rocks plot mainly in the basaltic andesite, andesite, trachyandesite and trachydacite fields (Figure 3a). On a K_2O-SiO_2 diagram (Peccerillo & Taylor 1976), the basaltic andesites and andesites belong to medium- to high-K series, whereas the trachyandesites and trachydacites fall in the high-K series field (Figure 3b).

On Harker diagrams (Figure 4), analyzed samples generally exhibit negative correlations between SiO_2 and CaO, MgO, $Fe_2O_3^T$, Al_2O_3, P_2O_5, TiO_2 and Sr and positive correlations between SiO_2 and K_2O, Na_2O_3, Zr, Ba, Rb, Nb, Th (Figure 4a–n). Basaltic andesites have higher CaO, $Fe_2O_3^T$, Al_2O_3 and Sr, whereas trachydacites have higher K_2O, Zr, Rb, Nb and Th contents than andesites and trachydacites (Figure 4). Compared to the Kale (Gümüşhane) volcanics the Torul volcanics have higher K_2O and Ba and lower CaO, $Fe_2O_3^T$, Al_2O_3, TiO_2 and Y concentrations (Figure 4a, c, e, f, h, j & o). For some major and trace elements, a noticeable variation in concentration exists as a function of geographic location. K_2O, Zr and Ba (Figure 4a, i & j) progressively increase from the southeast (Kale area) to the northwest (Torul area). In contrast, CaO, MgO, Fe_2O_3, Al_2O_3, TiO_2 and Sr tend to decrease from southeast to northwest.

Primitive mantle-normalized spider diagrams are shown in Figure 5a. All rocks exhibit significant enrichment in large ion lithophile elements (LILE) (Ba, Th, and K) relative to some high field strength elements (HFSE, such as Nb, Ta, P and Ti) and prominent positive Pb anomalies. All volcanic rocks show moderately fractionated chondrite-normalized REE patterns, parallel to each other (Figure 5b), indicating a similar source(s) for basaltic andesites, andesites, trachyandesites, and trachydacites. The

Table 2. K-Ar analytical data for the Torul volcanic rocks.

Sample	Rock type	Mineral	Ages (Ma)	± σ	K (%)	^{40}Ar rad (%)	^{38}Ar (10^{-11} mol)	$^{40}Ar/^{38}Ar$	± σ	$^{36}Ar/^{38}Ar$	± σ	$^{40}Ar*/^{40}K$	± σ
9	Bsa	hb	43.99	2.59	0.539	21.22	2.09E-11	0.555315	0.005142	0.001509	8.30E-07	0.002588	0.000154
13	And	hb	40.39	2.54	0.847	25.99	2.09E-11	0.638363	0.000769	0.001630	2.56E-05	0.002373	0.000151
4	Trd	hb	33.45	2.32	0.671	21.99	2.09E-11	0.503994	0.000288	0.001357	2.03E-05	0.001962	0.000137

λ= 5.543×10^{-10}/year, ^{40}K/ΣK= 1.167×10^{-4}, Bsa– basaltic andesite, And– andesite, Trd– trachydacite, hb– hornblende

Table 3. Whole-rock major (wt%) and trace (ppm) element analyses and CIPW norms of representative samples from the Torul volcanic rocks.

Rock Types	Basaltic andesite			Andesite			Trachyandesite			Trachydacite		
Sample	17	9	12	15	13	5	14	10	8	3	2	4
SiO_2	54.16	54.73	55.35	57.20	57.25	60.10	56.85	57.87	58.88	61.84	63.65	61.96
TiO_2	0.63	0.53	0.57	0.59	0.60	0.52	0.59	0.50	0.55	0.54	0.51	0.47
Al_2O_3	17.53	17.17	16.44	14.96	16.51	14.61	16.04	16.90	15.84	16.03	15.63	16.52
$Fe_2O_3^T$	8.10	6.88	6.90	7.30	5.86	6.10	6.69	6.09	6.53	5.54	5.11	4.76
MnO	0.15	0.13	0.13	0.14	0.10	0.08	0.09	0.30	0.11	0.08	0.09	0.07
MgO	4.04	3.86	3.79	4.45	4.48	3.86	3.11	2.92	3.21	1.80	1.59	1.66
CaO	8.64	8.07	8.25	7.51	6.53	6.63	6.52	4.99	5.22	3.27	3.26	4.22
Na_2O	3.02	2.97	2.61	3.02	3.85	2.83	3.30	3.72	3.02	4.96	3.72	3.42
K_2O	0.59	1.69	1.51	2.29	1.55	2.85	3.59	3.42	3.44	4.07	4.35	4.35
P_2O_5	0.23	0.17	0.22	0.22	0.21	0.22	0.19	0.14	0.18	0.19	0.18	0.14
LOI	2.70	3.50	3.90	2.10	2.80	1.90	2.80	2.90	2.70	1.50	1.70	2.20
Total	99.79	99.70	99.67	99.78	99.74	99.70	99.77	99.75	99.68	99.82	99.79	99.77
Ga	13.10	15.50	14.90	13.10	14.50	12.90	12.70	14.50	14.10	14.50	13.60	14.10
Ni	6.60	6.10	5.60	13.50	7.00	16.00	9.00	6.20	5.90	7.90	7.70	6.40
V	190.00	170.00	178.00	185.00	176.00	151.00	168.00	154.00	158.00	153.00	136.00	123.00
Cu	63.80	58.90	168.80	23.80	40.70	15.80	26.60	20.40	42.60	25.50	24.90	53.00
Pb	3.50	13.50	10.80	9.10	12.00	11.10	12.40	11.40	11.50	13.80	11.60	11.20
Zn	30.00	40.00	43.00	58.00	42.00	39.00	74.00	43.00	52.00	40.00	36.00	36.00
W	0.50	0.50	0.60	0.60	0.70	0.70	0.90	3.00	0.50	1.20	1.00	1.20
Rb	31.70	49.20	25.30	62.70	57.30	32.78	72.90	26.20	76.10	97.90	101.90	92.70
Ba	407.00	676.00	755.00	625.00	654.00	1138.00	730.00	1382.00	1262.00	841.00	920.00	961.00
Sr	782.40	814.10	927.80	436.60	480.20	462.40	458.00	641.30	703.80	386.90	325.50	588.90
Ta	0.30	0.30	0.30	0.20	0.30	0.30	0.30	0.30	0.30	0.30	0.40	0.30
Nb	2.40	3.90	4.40	2.20	4.30	4.30	4.20	4.30	4.40	5.00	5.10	5.40
Hf	1.70	2.60	3.20	1.40	2.20	2.40	2.40	2.70	2.50	3.60	3.30	3.30
Zr	64.40	76.20	96.90	58.60	86.50	82.30	90.80	96.60	98.40	121.40	113.90	122.40
Y	14.30	12.90	14.10	11.80	13.40	11.10	13.30	10.70	13.50	17.00	17.50	14.20
Th	2.90	7.50	8.00	5.00	7.10	6.80	6.80	9.10	7.60	8.80	8.60	10.10
U	1.20	2.30	2.80	1.00	2.40	2.10	1.70	2.50	2.60	2.60	2.80	2.50
Q	12.27	10.57	13.91	12.01	10.47	16.03	8.53	9.37	13.70	9.37	16.84	14.87
Or	3.49	9.99	8.92	13.53	9.16	16.84	21.22	20.21	20.33	24.05	25.71	25.71
Ab	25.55	25.13	22.09	25.55	32.58	23.95	27.92	31.48	25.55	41.97	31.48	28.94
An	32.53	28.53	28.68	20.50	23.19	18.74	18.35	19.31	19.50	9.45	13.10	16.88
Di	5.88	7.38	7.61	10.96	5.00	9.06	8.82	3.42	3.27	3.31	0.59	1.69
Hy	7.34	6.20	5.91	6.00	8.84	5.42	3.66	5.69	6.48	2.95	3.69	3.35
Ol	0.00	0.00	0.00	0.00	0.00	0.00	0.00	0.00	0.00	0.00	0.00	0.00
He	8.10	6.88	6.90	7.30	5.86	6.10	6.69	6.09	6.53	5.54	5.11	4.76
Il	0.32	0.28	0.28	0.30	0.21	0.17	0.19	0.64	0.24	0.17	0.19	0.15
Ap	0.53	0.39	0.51	0.51	0.49	0.51	0.44	0.32	0.42	0.44	0.42	0.32
Zr	0.01	0.01	0.01	0.01	0.01	0.01	0.01	0.01	0.01	0.03	0.03	0.03
Sph	1.13	0.94	1.04	1.06	1.20	1.05	1.20	0.40	1.05	1.10	1.00	0.96
Mg#	33.28	35.94	35.45	37.87	43.33	38.76	31.73	32.41	32.96	24.52	23.73	25.86
K/Na	0.20	0.57	0.58	0.76	0.40	1.01	1.09	0.92	1.14	0.82	1.17	1.27
Ba/La	39.13	32.04	36.65	45.62	35.16	63.58	46.50	70.51	62.17	39.12	44.66	41.78
Ba/Nb	169.58	173.33	171.59	284.09	152.09	264.65	173.81	321.40	286.82	168.20	180.39	177.96
Ce/Pb	5.97	2.70	3.53	2.92	2.96	2.80	2.43	2.89	3.36	2.87	3.38	3.65
La/Yb	5.78	13.53	13.73	9.07	12.48	12.97	10.06	13.33	13.62	9.39	9.58	13.07
Nb/La	0.23	0.18	0.21	0.16	0.23	0.24	0.27	0.22	0.22	0.23	0.25	0.23
Nb/Y	0.17	0.30	0.31	0.19	0.32	0.39	0.32	0.40	0.33	0.29	0.29	0.38
Sr/Y	54.71	63.11	65.80	37.00	35.84	41.66	34.44	59.93	52.13	22.76	18.60	41.47
Zr/Nb	26.83	19.54	22.02	26.64	20.12	19.14	21.62	22.47	22.36	24.28	22.33	22.67

$Fe_2O_3^T$ is total iron as Fe_2O_3, LOI is loss on ignition, Mg# (mg-number)= 100xMgO/(MgO+ $Fe_2O_3^T$), K/Na= K_2O/Na_2O

Coordinates of samples:
2: 00522351E-04486301N; 3: 00522466E-04486273N; 4: 00523952E-04486391N; 5: 00524105E-04486730N; 8: 00529482E-04485734N; 9: 00531318E-0794870N; 10: 00531768E-04481583N; 12: 00530930E-04484034N; 13: 00530587E-04485050N; 14: 00536322E-04483881N; 15: 00539386E-04480519N; 17: 00539550E-04479651N

Table 4. Rare earth elements analyses (ppm) from the Torul volcanic rocks.

Rock Types	Basaltic andesite			Andesite			Trachyandesite			Trachydacite		
Sample	17	9	12	15	13	5	14	10	8	4	3	2
La	10.40	21.10	20.60	13.70	18.60	17.90	15.70	19.60	20.30	23.00	21.50	20.60
Ce	20.90	36.40	38.10	26.60	35.50	31.10	30.10	33.00	38.60	40.90	39.60	39.20
Pr	2.81	4.38	4.66	3.49	4.43	4.00	3.92	4.11	4.65	4.97	5.21	4.87
Nd	12.40	17.10	18.70	14.50	20.30	12.16	16.90	15.97	19.20	18.30	20.70	19.80
Sm	2.94	3.24	3.82	3.41	3.84	2.88	3.41	3.18	3.39	3.38	3.85	3.53
Eu	0.88	1.00	1.13	1.02	1.16	0.95	0.96	0.97	1.08	0.94	1.08	0.95
Gd	2.80	3.27	3.60	3.47	3.46	2.70	3.01	2.80	3.19	3.11	3.59	3.56
Tb	0.38	0.37	0.43	0.39	0.42	0.32	0.39	0.35	0.40	0.39	0.50	0.41
Dy	3.04	2.72	2.79	3.02	2.81	2.20	3.06	2.31	2.59	2.62	3.06	2.88
Ho	0.51	0.45	0.47	0.45	0.52	0.45	0.50	0.44	0.49	0.51	0.62	0.55
Er	1.70	1.44	1.51	1.39	1.50	1.22	1.69	1.38	1.60	1.51	2.03	2.02
Tm	0.25	0.21	0.23	0.22	0.23	0.19	0.24	0.21	0.23	0.25	0.35	0.30
Yb	1.80	1.56	1.50	1.51	1.49	1.38	1.56	1.47	1.49	1.76	2.29	2.15
Lu	0.27	0.23	0.25	0.19	0.22	0.19	0.24	0.21	0.22	0.25	0.38	0.31
$(La/Lu)_{cn}$	3.99	9.50	8.53	7.47	8.75	9.75	6.77	9.66	9.55	9.53	5.86	6.88
$(La/Sm)_{cn}$	2.23	4.10	3.39	2.53	3.05	3.91	2.90	3.87	3.77	4.28	3.51	3.67
$(Gd/Lu)_{cn}$	1.29	1.77	1.79	2.27	1.95	1.76	1.56	1.66	1.80	1.54	1.17	1.43
$(La/Yb)_{cn}$	3.90	9.14	9.28	6.13	8.44	8.77	6.80	9.01	9.21	8.83	6.34	6.47
$(Tb/Yb)_{cn}$	0.90	1.01	1.23	1.10	1.21	0.99	1.07	1.02	1.15	0.95	0.93	0.82
Eu_N/Eu^*	0.92	0.93	0.92	0.90	0.95	1.03	0.90	0.97	0.99	0.87	0.87	0.81

$Eu^*=(Sm+Gd)_{cn}/2$

(La_N/Lu_N) ratios vary between 4 and 10 in the basaltic andesites, and between 6 and 10 in the trachydacites (Table 4). The basaltic andesites show weak negative Eu-anomalies ($Eu_N/Eu^* = 0.92–0.93$). The slight increase of the negative Eu-anomaly from these rocks towards the trachydacites ($Eu_N/Eu^* = 0.81–0.87$) indicates a genetic link between the mafic and felsic rock types. As seen from Figure 5, the Torul volcanics are somewhat similar to the Kale lavas (Arslan & Aliyazıcıoğlu 2001) in the chondrite-normalized REE and trace element concentration diagrams, with the Torul volcanics more enriched in LILE and LREE than the Kale volcanics.

Sr and Nd Isotope Geochemistry

Sr and Nd isotope compositions of the Torul volcanic rocks are listed in Table 5. Initial $^{87}Sr/^{86}Sr$ and $^{143}Nd/^{144}Nd$ ratios were calculated using an age of 43 Ma based on the results of K-Ar dating. The Torul volcanics display relatively homogeneous isotopic compositions. All samples show a small range of Sr-Nd isotope ratios (initial $^{87}Sr/^{86}Sr$ ratios from 0.70457 to 0.70511 and $^{143}Nd/^{144}Nd$ ratios from 0.51264 to 0.51278). For the most primitive basaltic andesite samples, $^{87}Sr/^{86}Sr_{(i)}$ ratios range from 0.70457 to 0.70501 and $^{143}Nd/^{144}Nd_{(i)}$ ratios range from 0.51264 to 0.51278; for the most evolved trachydacitic samples, $^{87}Sr/^{86}Sr_{(i)}$ ratios are 0.70511 and $^{143}Nd/^{144}Nd_{(i)}$ ratios are 0.51269. In the Sr and Nd isotope correlation diagram (Figure 6), the Torul volcanics are placed on the mantle array in between the depleted and the enriched quadrants. For comparison, samples from other Tertiary to Quaternary calc-alkaline volcanic suites of eastern Anatolia, central Anatolia and eastern Pontides are also plotted in Figure 6. The Torul volcanic rocks have higher $^{87}Sr/^{86}Sr_{(i)}$ ratios than the eastern Anatolian calc-alkaline volcanic rocks and lower $^{87}Sr/^{86}Sr_{(i)}$ ratios than central Anatolian calc-alkaline volcanic rocks (Figure 6).

Discussion

Petrogenetic Consideration

The geochemical features of the Torul volcanics (depletion of Nb, Zr and Ta, enrichment of Sr, K, Rb and Ba, and high Ba/La ratios) are typical of subduction zone volcanic rocks (cf. Thompson *et al.* 1984; White & Patchett 1984; Elburg *et al.* 2002). The
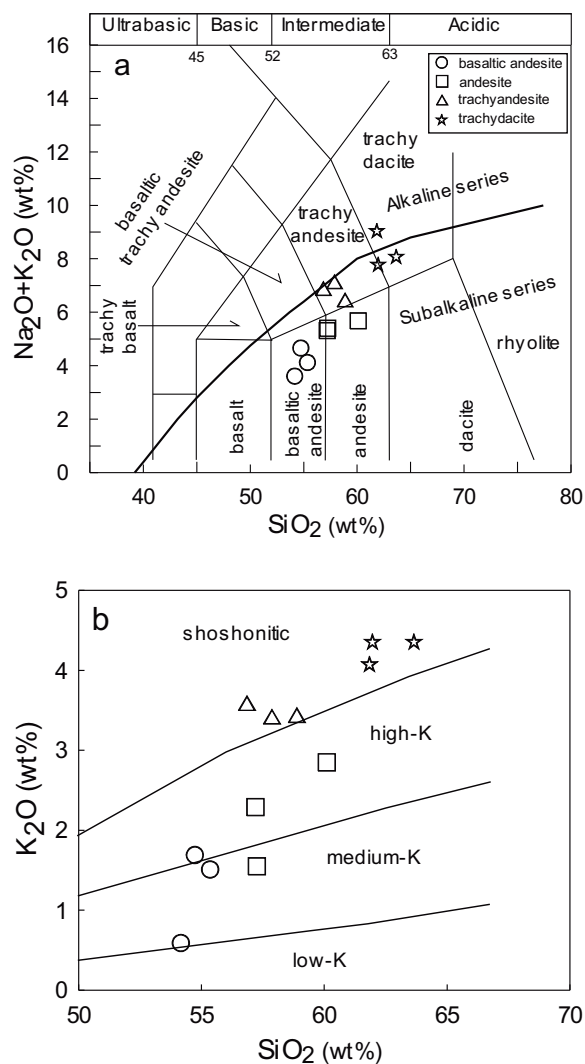
Figure 3. (a) Chemical classification diagram (Le Maitre *et al.* 2002); alkaline-subalkaline dividing line is from Irvine & Baragar (1971); **(b)** K_2O vs SiO_2 diagram of the Torul volcanic rocks with field boundaries between medium-K, high-K and shoshonitic series after Peccerillo & Taylor (1976).

most basic samples (basaltic andesite) have low MgO and Ni contents, suggesting that they do not represent primary magma compositions. The basaltic and andesitic rocks, similar to orogenic andesites, have higher Ba/La (32.0–70.5) and lower Nb/La (0.16–0.27) ratios compared to MORB, OIB, and intra-plate basalts (Sun & McDonough 1989), indicating a different origin and geodynamic evolution. The geochemical, Sr and Nd isotopic

compositions of the Torul volcanic rocks provide constraints on the evolution processes of the parental magma and the nature of the mantle source. These processes will be discussed in the following sections.

Fractional Crystallization

The Torul volcanic rocks have similar petrographical and geochemical features, and define a typical K-rich calc-alkaline trend from basaltic andesites to trachydacites. Major and trace element abundances vary along continuous trends of decreasing MgO, CaO, TiO_2, $Fe_2O_3^T$ and Sr, and increasing K_2O, Rb, Zr, Nb and Th with increasing SiO_2 (Figure 4). Normalized REE patterns of the Torul volcanics are parallel to each other and total REE contents increase from basaltic andesite to trachydacite (Figure 5b). The increases in SiO_2, K_2O, Rb, Ba and decreases in TiO_2, P_2O_5, CaO, MgO, $Fe_2O_3^T$, and Al_2O_3 contents shown in the basaltic andesites and trachydacites are compatible with their evolution by fractional crystallization (Figure 4). Decrease in P_2O_5 may result from removal of apatite during fractional crystallization. The negative Eu anomalies and the decrease in Sr with increase in silica, all assert that plagioclase was an important fractionating phase. The increases in K_2O and Rb with increasing silica content indicate that K-feldspar and biotite were not among the early phases of fractionation. Additionally, the downward-concave shape of the REE pattern suggests a significant role of clinopyroxene and hornblende fractionation in the evolution of the rocks, as also confirmed by petrography (Figure 5b).

The fractionation crystallization model has been tested by a Y versus Rb plot (Pearce *et al.* 1990; Figure 7a), using Rb as a fractionation index, since Rb has a positive correlation with increasing silica content throughout the fractionation process. The Y content of the samples exhibits a near-constant to positive correlation with increasing Rb contents, which can be explained by plagioclase and clinopyroxene fractionation (Figure 7a).

For calc-alkaline volcanic suites, Lambert & Holland (1974) used a CaO versus Y diagram to define J- and L-type trends, which lead to depletion and enrichment in Y relative to a calc-alkaline series
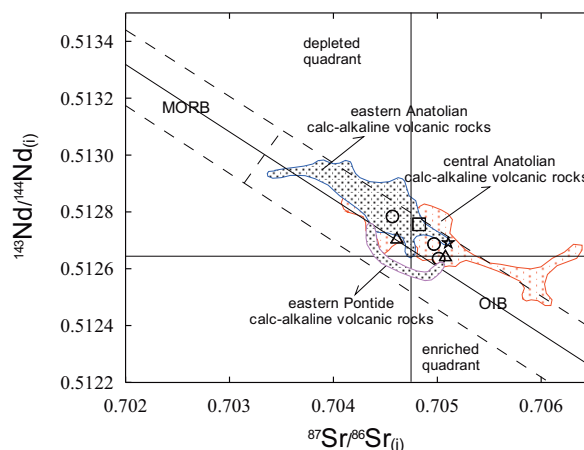
147
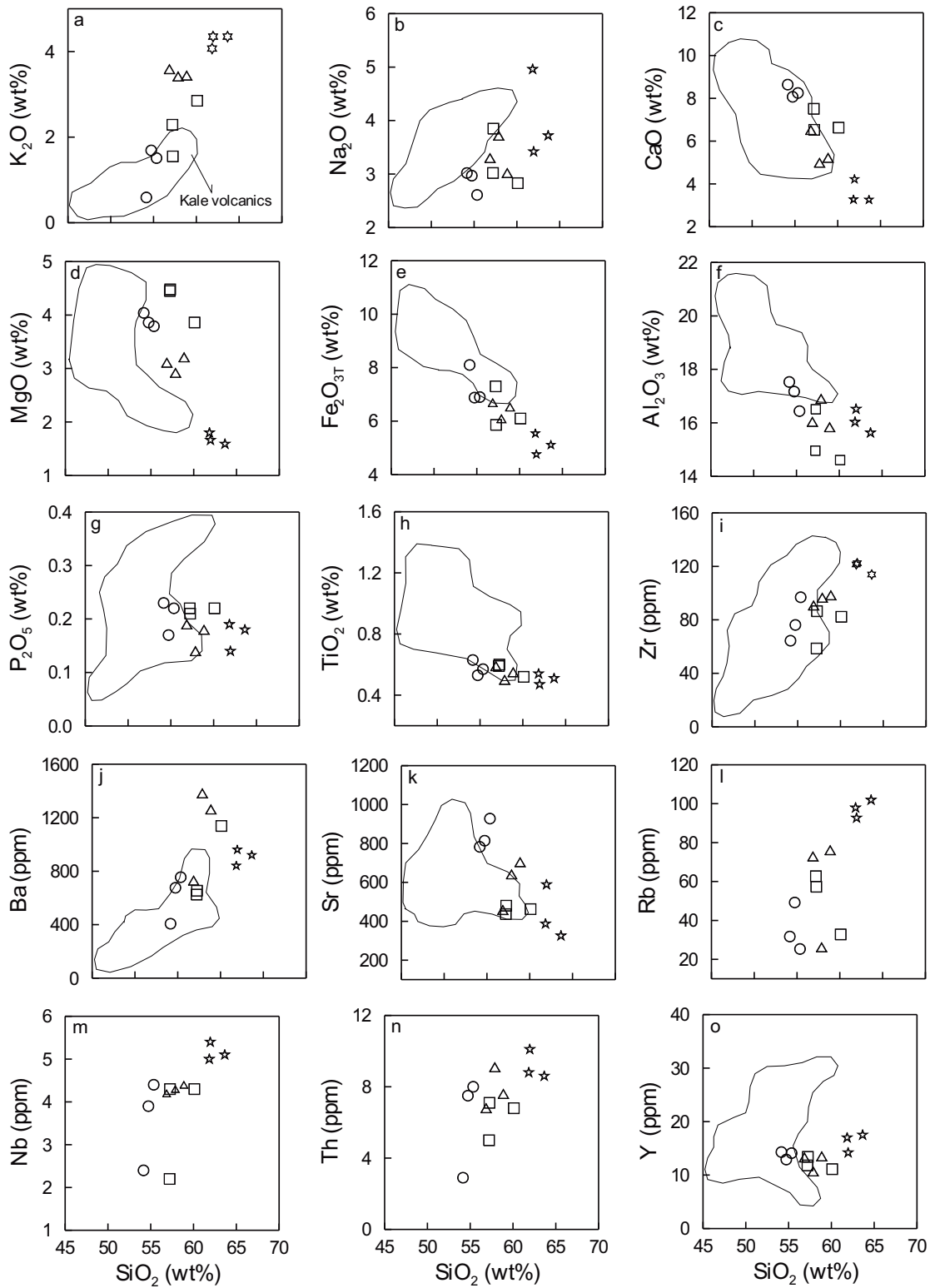
Figure 4. (a–o) SiO$_2$ (wt%) versus major oxides (wt %) and trace elements (ppm) variation diagrams for samples from the Torul volcanic rocks. Fields for the Kale (Gümüşhane) volcanics (Arslan & Aliyazıcıoğlu 2001) in the eastern Pontides collision-related volcanic province are plotted for comparison. For symbols, see Figure 3.

Figure 6. $^{87}Sr/^{86}Sr_{(i)}$ vs. $^{143}Nd/^{144}Nd_{(i)}$ diagram from the Torul volcanic rocks. Also plotted for comparison are the samples from other Tertiary to Quaternary calc-alkaline volcanic rocks of Turkey, including the eastern Anatolian calc-alkaline volcanic rocks (Pearce *et al.* 1990; Buket & Temel 1998; Keskin *et al.* 2006; Kaygusuz 2009), the central Anatolian calc-alkaline volcanic rocks (Deniel *et al.* 1998; Temel *et al.* 1998; Yalçın *et al.* 1998; Şen *et al.* 2004; Varol *et al.* 2007; Kurt *et al.* 2008), and the eastern Pontide calc-alkaline volcanic rocks (Temizel 2008). MORB– mid-ocean ridge basalts; OIB– ocean island basalts. For symbols, see Figure 3.

Figure 5. (a) Primitive mantle normalized trace element patterns (normalizing values from Sun & McDonough 1989); **(b)** chondrite normalized rare earth element patterns (normalizing values from Taylor & McLennan 1985) for samples from the Torul volcanic rocks. Fields for the Kale (Gümüşhane) volcanics (Arslan & Aliyazıcıoğlu 2001) in the eastern Pontides collision-related volcanic province are plotted for comparison. N-MORB is from Saunders & Tarney (1984), OIB is from Sun & McDonough (1989). For symbols, see Figure 3.

Crustal Assimilation

standard, respectively. The J- and L-type trends have been termed hornblende (± garnet) and pyroxene controlled differentiation trends, respectively, as these minerals can be critical in determining the trend direction. In the Y versus CaO plot (Figure 7b), nearly all rocks plot on the Y enrichment side (high-Y content) of the standard calc-alkaline trend, defining an L-type trend. This trend suggests that pyroxene and plagioclase played an important role in the evolution of the studied volcanics.

Many studies on arc magmatism attest to the importance of crustal assimilation, which leads to modification of the trace element and isotopic composition of mantle-derived arc magmas (i.e. Ellam & Harmon 1990; Thirlwall *et al.* 1996; Hochstaedter *et al.* 2000; McDermott *et al.* 2005; Zellmer *et al.* 2005). Temizel & Arslan (2003, 2005) argued for contamination of the primary melt by arc crust as an important feature in Tertiary lavas of the eastern Pontides. However, Arslan *et al.* (2007a) and Temizel (2008) found minor evidence for assimilation and fractional crystallization (AFC) processes in Tertiary volcanics of the southern Pontide zone and suggested that the composition of these rocks was mainly modified by fractional crystallization rather than AFC. The Torul volcanic rocks were erupted through a thickened arc crust making them more susceptible to modification by crustal assimilation. The continental crust has highly fractionated and enriched LREE, flat HREE, and a positive Pb anomaly but negative Nb-Ta anomalies

Table 5. Sr and Nd isotope data from the Torul volcanic rocks.

Sample	Rb (ppm)	Sr (ppm)	$^{87}Rb/^{86}Sr$	$^{87}Sr/^{86}Sr$	(2σ)	$(^{87}Sr/^{86}Sr)_{43Ma}$	Sm (ppm)	Nd (ppm)	$^{147}Sm/^{144}Nd$	$^{143}Nd/^{144}Nd$	(2σ)	$(^{143}Nd/^{144}Nd)_{43Ma}$	$\varepsilon Nd(i)$[a]	$\varepsilon Nd(0)$[a]	T_{DM}[b] (Ga)	T_{DM}[c] (Ga)
Basaltic andesite																
17	31.7	782	0.11750	0.704640	8	0.70457	2.94	12.40	0.14334	0.512824	7	0.51278	3.92	3.63	0.66	0.53
9	49.2	814	0.17526	0.705075	8	0.70497	3.24	17.10	0.11455	0.512719	6	0.51269	2.03	1.58	0.63	0.69
12	25.3	927	0.07908	0.705061	9	0.70501	3.82	18.70	0.12350	0.512670	8	0.51264	1.03	0.62	0.77	0.77
Andesite																
5	32.8	462	0.20558	0.704951	7	0.70483	2.88	12.16	0.14306	0.512796	7	0.51276	3.38	3.09	0.71	0.58
Trachyandesite																
8	76.1	703	0.31357	0.705270	8	0.70508	3.39	19.20	0.10674	0.512677	7	0.51265	1.25	0.76	0.64	0.75
10	26.2	641	0.11848	0.704683	7	0.70461	3.18	15.97	0.12052	0.512743	7	0.51271	2.47	2.05	0.63	0.65
Trachydacite																
4	92.70	588.90	0.45650	0.705384	9	0.70511	3.38	18.30	0.11166	0.512722	6	0.51269	2.11	1.64	0.61	0.68

[a] $\varepsilon Nd(i)$ and $\varepsilon Nd(0)$ values are calculated based on present-day $^{147}Sm/^{144}Nd= 0.1967$ and $^{143}Nd/^{144}Nd= 0.512638$

[b] Single stage model age (T_{DM}), calculated with depleted mantle present-day parameters $^{143}Nd/^{144}Nd= 0.513151$ and $^{147}Sm/^{144}Nd= 0.219$

[c] Two-stage model age (T_{DM}), according to Liew & Hoffman (1988)
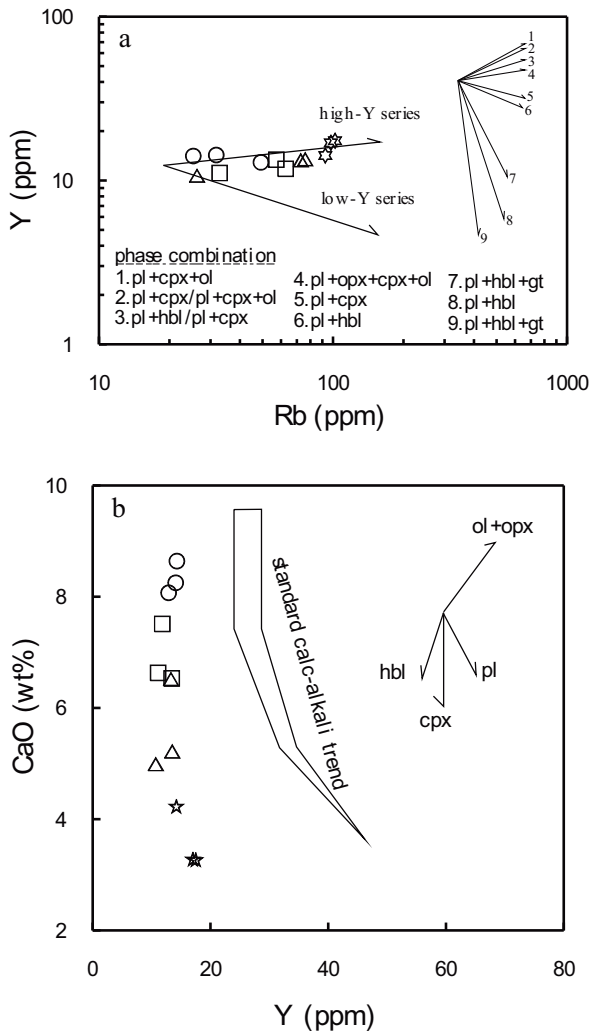
Figure 7. (a) Rb vs Y diagram showing crystallization of the phase combinations between the plagioclase-olivine-pyroxene-magnetite dominated fractionation trends and plagioclase-amphibole dominated fractionation trend (Pearce *et al.* 1990); (b) Y vs CaO diagram, compared with the standard calc-alkaline trend of Lambert & Holland (1974) from the Torul volcanic rocks. For symbols, see Figure 3.

(Taylor & McLennan 1985). The Torul volcanic rocks are characterized by pronounced negative Nb–Ta and positive Pb anomalies (Figure 5a), recording a subduction signature and possible minor crustal contribution in their evolution.

In Figure 8, the $^{87}Sr/^{86}Sr_{(i)}$ and $^{143}Nd/^{144}Nd_{(i)}$ ratios are plotted against SiO_2, MgO, Rb/Sr, Th, Sr, Sm/Nd and Nd to evaluate the role of fractional crystallization (FC) or AFC processes. Positive or negative trends indicate that the magmas were affected by AFC processes, whereas nearly constant trends indicate significant fractional crystallization. $^{87}Sr/^{86}Sr_{(i)}$ contents of the Torul samples vs SiO_2, Rb/Sr, Sr, and $^{143}Nd/^{144}Nd_{(i)}$ contents vs SiO_2 and MgO exhibit near–constant trends. $^{87}Sr/^{86}Sr_{(i)}$ and $^{143}Nd/^{144}Nd_{(i)}$ contents show some positive correlation with Th, Sm/Nd, but a negative correlation appears for $^{87}Sr/^{86}Sr_{(i)}$ vs MgO and for $^{143}Nd/^{144}Nd_{(i)}$ vs Nd. All of these trends indicate that the calc–alkaline rocks in the Torul area were generated from similar subduction–induced sources and fractional crystallization rather than AFC mainly controls the compositional differences, which is consistent with the finding of Arslan *et al.* (2007a) and Temizel (2008).

Source Characteristics

The overall enrichments in LILE and LREE and the negative Nb-Ta-Ti anomalies are features of subduction-related magmas and are commonly attributed to a mantle source that was modified by metasomatic fluids derived from the subducted slab or sediments (e.g., Pearce 1983; Hawkesworth *et al.* 1997; Elburg *et al.* 2002). We suggest that the trace element characteristics of the Torul volcanics originate from melting of enriched subcontinental mantle, modified by earlier (pre-Eocene) subduction processes.

The Torul volcanics show relatively high and flat HREE patterns (Figure 5b), pointing to the absence of garnet in the mantle source region. Instead, the patterns are consistent with the presence of spinel in the mantle source. The depletion in Nb, Ta and Ti can be explained by their retention in Ti-rich residual mineral phases (Foley & Wheller 1990; Pearce & Parkinson 1993). The negative P and Zr anomalies in the primitive mantle-normalized diagrams (Figure 5a) could reflect the presence of residual apatite and zircon in the mantle source region (Guo *et al.* 2006) or fractionation of these mineral phases during later petrogenetic processes. Furthermore, the relative HFSE depletion with respect to LILE may also be explained with a mantle source modified by subduction-related fluids, and thus LILE enriched. This may explain Nb, Ta, Ti and Zr depletion in the studied volcanics.

A Th/Y-Nb/Y plot (Figure 9a) may provide some useful constraints concerning potential source components involved in the petrogenesis of the

151
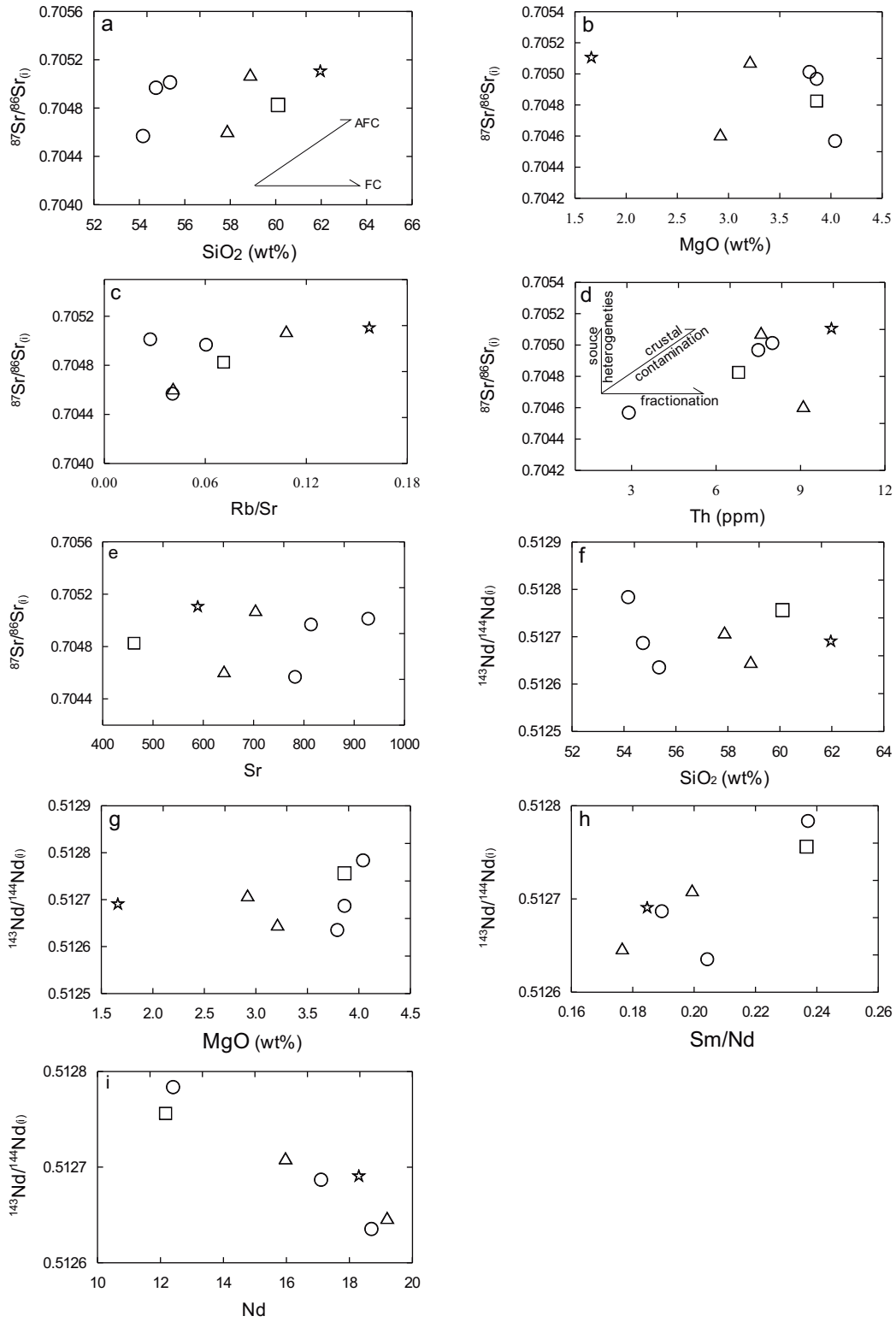
Figure 8. (a–i) Variation diagrams of $^{87}Sr/^{86}Sr_{(i)}$ and $^{143}Nd/^{144}Nd_{(i)}$ vs. SiO_2, MgO, Rb/Sr, Th, Sr, Sm/Nd and Nd from the Torul volcanic rocks. For symbols, see Figure 3.
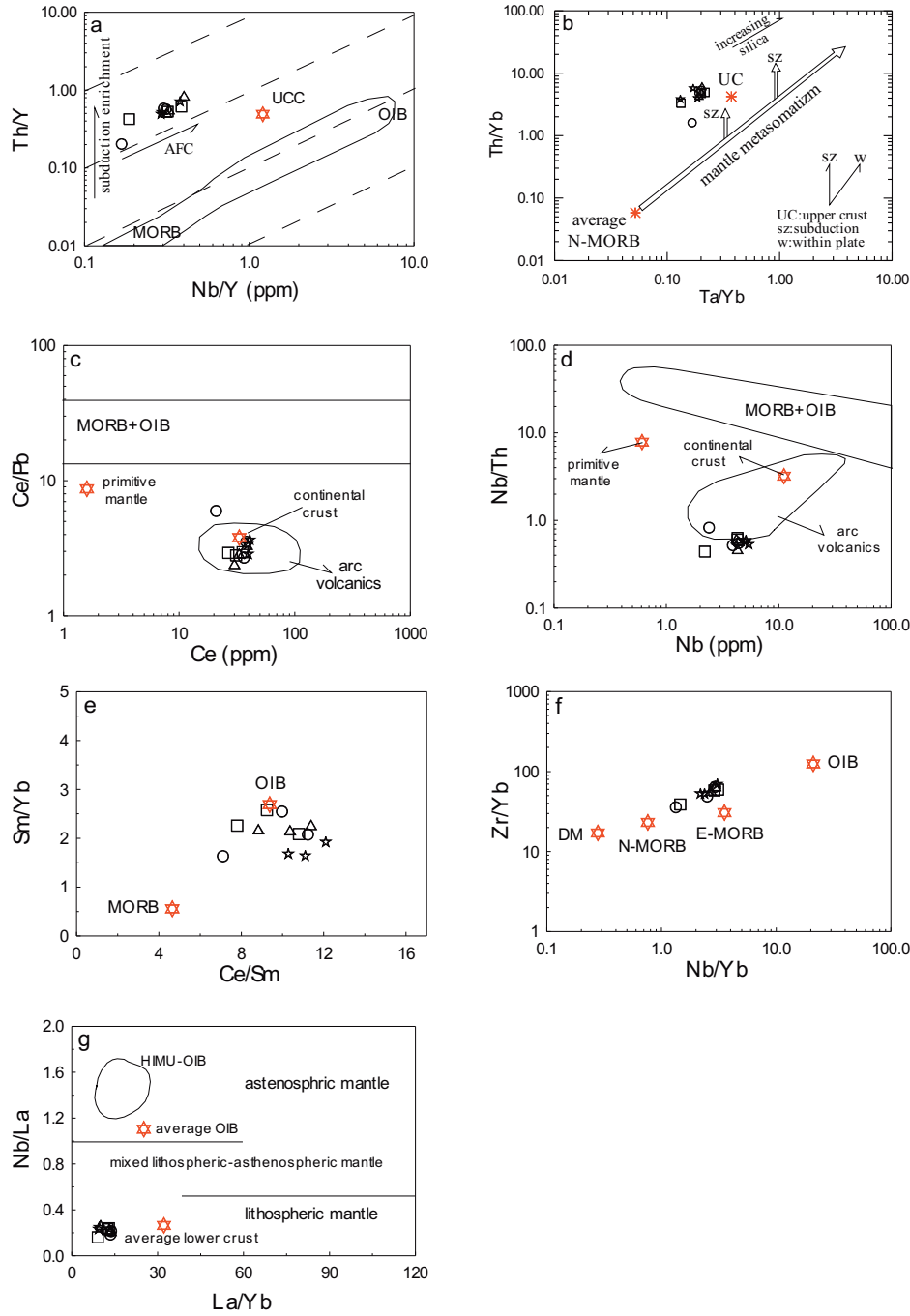
Figure 9. (a) Th/Y vs Nb/Y (Pearce 1983); (b) Th/Yb vs Ta/Yb; (c) Ce/Pb vs Ce; (d) Nb/Th vs Nb; (e) Sm/Yb vs Ce/Sm (Pearce 1982); (f) Zr/Yb vs Nb/Yb (Pearce & Peate 1995); (g) Nb/La vs La/Yb plots of the rock samples from the Torul volcanic rocks. Compositions of the upper crusts after Taylor & McLennan (1985) in (a). Primitive mantle after Hoffmann (1988) in (c); compositions of continental crust, mid-ocean ridge basalts (MORB), ocean-island basalts (OIB) and arc volcanics after Schmidberger & Hegner (1999) in (c) & (d). The compositions of MORB and OIB after Harms *et al.* (1997) in (e). The DM (depleted mantle), N-MORB, E-MORB, OIB compositions after Sun & McDonough (1989) in (f). Average OIB is after Fitton *et al.* (1991) and average lower crust is after Chen & Arculus (1995) in (g). Dashed lines separating fields of the asthenospheric, lithospheric and mixed mantle are plotted based on data given in Smith *et al.* (1999) in (g). The HIMU-OIB area is reported in Weaver *et al.* (1987) in (g). For symbols, see Figure 3.

magmas (Wilson *et al.* 1997). The Torul volcanics define a coherent trend, with a Th/Nb ratio close to 0.1, which may be attributed to the combined effects of fractional crystallization and crustal assimilation. The displacement of this data array to higher Th/Y ratios compared to MORB and OIB is strongly indicative of metasomatism of the mantle source by subduction zone fluids carrying the trace element signature of a crustal component. The Th/Yb vs Ta/Yb (Pearce *et al.* 1990, Figure 9b) diagram may be used to display source variation and crustal contamination. In this diagram, the Torul volcanic rocks form a trend sub–parallel to the mantle array but shifted to higher Th/Yb ratios. This suggests melt derivation from a source, which had been previously enriched (or metasomatized) by fluids derived from an earlier (i.e. pre-Eocene) subduction processes (e.g., Arslan *et al.* 2007a; Temizel & Arslan 2008).

The source characteristics of the Torul volcanic rocks can be better investigated using specific trace element diagrams (Figure 9c–f). In the Ce/Pb vs Ce and Nb/Th vs Nb diagrams (Figure 9c, d) all samples plot in the arc volcanic subfield. The average low Ce/Pb ratios (~5) of the most primitive samples differ considerably from those of oceanic basalts (~25; Hoffmann 1988), suggesting that these rocks are not derived from normal asthenospheric mantle. The Sm/Yb vs Ce/Sm diagram (Figure 9e) indicates an apparent OIB-like enriched mantle composition rather than a depleted MORB-like composition for almost all samples. In the Nb/Yb vs Zr/Yb diagram (Figure 9f), samples plot within the general MORB-OIB trend.

Bradshaw & Smith (1994) and Smith *et al.* (1999) suggested that, since HFSE (such as Nb and Ta) are depleted in the lithospheric mantle relative to the LREE, high Nb/La ratios (~>1) indicate an OIB like asthenospheric mantle source for basaltic magmas, and lower ratios (~<0.5) indicate a lithospheric mantle source. The Nb/La (0.18–0.23) and La/Yb (5.8–13.7) ratios of the most basic samples in the Torul area suggest a lithospheric mantle source (Figure 9g). However, low Nb/La ratios can derive from a lithospheric source, but also from a La-enrichment in the source, given the metasomatization of mantle source by subduction fluids (evident on diagrams 9a and 9b), and given

that La mobility in fluids is notably higher that Nb mobility. Therefore, we suggest that low La/Nb ratios in Torul volcanics are here due to fluid-driven La enrichment in the mantle source, modified by slab-released fluids.

Sr and Nd isotope ratios for the Torul volcanics define a narrow field between bulk earth composition and depleted mantle (Figure 6, Table 5). Isotope ratios are very close to those of eastern Pontide calc–alkaline volcanics (Arslan *et al.* 2007; Temizel 2008). Furthermore, similar $^{87}Sr/^{86}Sr$ and $^{143}Nd/^{144}Nd$ isotope compositions support the genetic link between the mafic and more felsic rocks of the Torul volcanic suite via fractional crystallization (Figures 6 & 8).

Geodynamic Implications

The eastern Pontides constitute a Upper Mesozoic–Early Tertiary east–west-trending magmatic belt (Figure 1). This belt is interpreted as an island arc developed in response to the subduction of the Neo-Tethyan oceanic crust beneath the Eurasian plate (Yılmaz *et al.* 1997; Okay & Şahintürk 1997). Closure of the Neo-Tethyan Ocean caused a collision between the Pontide arc and the Tauride-Anatolide platform. Both the onset of subduction and the timing of collision between the Pontides and the Anatolide-Tauride platform is a matter of debate (e.g., Tokel 1977; Akın 1978; Robinson *et al.* 1995; Okay & Şahintürk 1997; Boztuğ *et al.* 2004). Subduction under the eastern Pontides is argued to have started either during the Jurassic (Adamia *et al.* 1977; Kazmin *et al.* 1986), or during the Cretaceous (Şengör & Yılmaz 1981; Görür 1988). During Palaeocene–Early Eocene time, the eastern Pontides was above sea-level (Okay & Şahintürk 1997). Based on structural data and the composition and timing of igneous activity, Şengör & Yılmaz (1981), Yılmaz *et al.* (1997), Okay & Şahintürk (1997), and Boztuğ *et al.* (2004) proposed a Paleocene–Early Eocene (ca. 55 Ma) collision, resulting in crustal thickening and regional uplift of the eastern Pontides. Tokel (1977), Akın (1978), and Robinson *et al.* (1995) considered that the Middle Eocene volcanic rocks formed during northward subduction of the eastern Pontides and collision occurred in the Oligocene (ca. 30 Ma).

The contrasting interpretations for the timing and mechanism of collision in the eastern Pontides largely result from considerations of Tertiary magmatism in this region. Arslan *et al.* (2001, 2002, 2007a, 2009) suggested that the eastern Pontides bear features of a thickening continental crust and the subduction-imposed thermal structure was very important in the generation of Tertiary magmatism.

Geochemical and isotope composition of the Torul volcanics is consistent with derivation from a subduction-enriched mantle source. Two different models exist that could explain the melting process of mantle during the Cenozoic: (1) melting by perturbation of the geotherm by heat from upwelling asthenospheric mantle (either by lithospheric delamination or by detachment of subducted slab), (2) melting of lithospheric mantle by adiabatic decompression resulting from lithospheric extension or uplift. There is no evidence for mantle upwelling beneath the Pontides terrane, which weakens the possibility that a plume-like mechanism caused the melting of the lithospheric mantle. Maden *et al.* (2009) interpreted the prominent E–W-, NE- and NW-trending lineaments of the eastern Pontides as important extensional tectonic structures of the Pontide crust. Moreover, Arslan *et al.* (2007a, b, 2009) suggested that Tertiary volcanism is closely related to lithospheric thinning induced by slab break-off. Thus, melting of the lithospheric mantle beneath the eastern Pontides during the Eocene seems more likely to have occurred by decompression melting of an enriched subduction modified mantle, which was metasomatized by fluids derived from pre-Eocene subduction zone processes (e.g., Arslan *et al.* 2007a; Temizel & Arslan 2008). Subsequently, these melts underwent a considerable degree of fractional crystallization along with minor amounts of crustal assimilation, generating the wide variety of rock types ranging from basaltic andesite to trachydacite.

Conclusions

- The studied Torul volcanic rocks vary from basaltic andesite to trachydacite defining a calc-alkaline series.

- K-Ar dating on hornblende separates from various lava flows gave ages between 44.0±2.6 and 33.5±2.3 Ma.

- The Torul volcanics have initial $^{87}Sr/^{86}Sr$ values varying between 0.70457 and 0.70511 and initial $^{143}Nd/^{144}Nd$ values between 0.51264 and 0.51278.

- All samples from the Torul volcanic series display similar geochemical features. They are characterized by enrichment of LILE and LREE and depletion of HFSE suggesting similar sources and petrogenetic processes.

- There is systematic spatial variation in K_2O, CaO, MgO, Fe_2O_3, Al_2O_3, TiO_2, Zr, Sr and Ba concentrations from the southeast (Kale area) to the northwest (Torul area).

- Fractional crystallization (FC) with minor amounts of crustal contamination occurred during the evolution of the volcanic rocks with pyroxene, hornblende, plagioclase and Fe-Ti oxides as the most important fractionating mineral phases.

- The Torul volcanic rocks were derived from an enriched mantle source, which was previously modified by subduction fluids in a post-collisional geodynamic setting.

References

ADAMIA, S.A., LORDKIPANIDZE, M.B. & ZAKARIADZE, G.S. 1977. Evolution of an active continental margin as examplified by the Alpine history of the Caucasus. *Tectonophysics* **40**, 183–199.

AKIN, H. 1978. Geologie, magmatismus und lager-staettenbidung imostpontischen Gebirge-Turkei aus der sicht der plattentektonik. *Geologische Rundschau* **68**, 253–283.

AKINCI, Ö.T. 1984. The eastern Pontide volcano-sedimentary belt and associated massive sulphide deposits. *In*: DIXON, J.E. & ROBERTSON, A.H.F. (eds), *The Geological Evolution of the Eastern Mediterranean*. Geological Society, London, Special Publications **17**, 415–428.

ALTHERR, R., TOPUZ, G., SIEBEL, W., ŞEN, C., MEYER, H.P, SATIR, M. & LAHAYE, Y. 2008. Geochemical and Sr-Nd-Pb isotopic characteristics of Paleocene plagioleucitites from the eastern Pontides (NE Turkey). *Lithos* **105**, 149–161.

ANDERSON, J.L. & SMITH, D.R. 1995. The effects of temperature and oxygen fugacity on the Al-in-hornblende barometry. *American Mineralogist* **80**, 549–559.

ARSLAN, M. & ALİYAZICIOĞLU, İ. 2001. Geochemical and petrological characteristics of the Kale (Gümüşhane) volcanic rocks: implications for the Eocene evolution of eastern Pontide arc volcanism, northeast Turkey. *International Geology Review* **43**, 595–610.

ARSLAN, M. & ASLAN, Z. 2006. Mineralogy, petrography and whole-rock geochemistry of the Tertiary granitic intrusions in the eastern Pontides, Turkey. *Journal of Asian Earth Sciences* **27**, 177–193.

ARSLAN, M., ASLAN, Z., ŞEN, C. & HOSKIN, P.W.O. 2000a. Constraints on petrology and petrogenesis of Tertiary volcanism in the eastern Pontide paleo-arc system, NE Turkey. *10th V.M. Goldschmidt Conference, Journal of Conference, Abstracts* **5**, 157–158.

ARSLAN, M., BOZTUĞ, D., ŞEN, C., KOLAYLI, H., TEMİZEL, İ. & ABDİOĞLU, E. 2007a. *Petrogenesis and Geodynamic Evolution of the Southern Zone Eocene Volcanism, eastern Pontides*. TÜBİTAK-ÇAYDAG Project no. **103Y012** [in Turkish with English abstract, unpublished].

ARSLAN, M., BOZTUĞ, D., TEMİZEL, İ., KOLAYLI, H., ŞEN, C., ABDİOĞLU, E., RUFFET, G. & HARLAVAN, Y. 2007b. $^{40}Ar/^{39}Ar$ geochronology and Sr-Pb isotopic evidence of post-collisional extensional volcanism of the eastern Pontide paleo-arc, NE Turkey. Special Supplement, 17th Annual V.M. Goldschmidt Conference, Geochronology of Tectonic Processes. *Geochimica et Cosmochimica Acta* **71**, 15S, A38.

ARSLAN, M., HOSKIN, P.W.O. & ASLAN, Z. 2001. Continental crust formation and thermal consequences of Cenozoic thickening of the eastern Pontides Tectonic unit: preliminary temporal constraints and implications. *Fourth International Turkish Geology Symposium, Adana-Turkey, Abstracts*, p. 121.

ARSLAN, M., ŞEN, C., ALİYAZICIOĞLU, İ., KAYGUSUZ, A. & ASLAN, Z. 2000b. Comparative geology, mineralogy and petrology of Eocene (?) volcanics in Trabzon and Gümüşhane areas (NE, Turkey). *Earth Science and Mining Conference, Journal of Conference Book* **1**, 39–53 [in Turkish with English abstract].

ARSLAN, M., TEMİZEL, İ. & ABDİOĞLU, E. 2002. Subduction input versus source enrichment and role of crustal thickening in the generation of Tertiary magmatism in the Pontide paleo-arc setting, NE Turkey. *In*: DE VIVO, B. & BODGAR, R.J. (eds), *Workshop-Short Course on Volcanic Systems, Geochemical and Geophysical Monitoring, Melt Inclusions: Methods, Applications and Problems, Napoli, Italy*, 13–16.

ARSLAN, M., TEMİZEL, İ., BOZTUĞ, D., ABDİOĞLU, E., KOLAYLI, H. & YÜCEL, C. 2009. Petrochemistry, ^{40}Ar-^{39}Ar geochronology and Sr-Pb isotope geochemistry of the Tertiary volcanics in eastern Pontide southern zone, NE Turkey: geodynamic evolution related to slab break-off and transtensional tectonics. *2. International Symposium on the Geology of the Black Sea Region Abstract Book*, p. 24.

ARSLAN, M., TÜYSÜZ, N., KORKMAZ, S. & KURT, H. 1997. Geochemistry and petrogenesis of the eastern Pontide volcanic rocks, Northeast Turkey. *Chemie der Erde* **57**, 157–187.

AYDIN, F. 2004. *Mineral Chemistry, Petrology and Petrogenesis of the Değirmendere Valley Volcanics (Trabzon-Esiroğlu, NE-Turkey)*. PhD Thesis, Karadeniz Technical University, Trabzon [in Turkish with English abstract, unpublished].

AYDIN, F., KARSLI, O. & CHEN, B. 2008. Petrogenesis of the Neogene alkaline volcanics with implications for post-collisional lithospheric thinning of the eastern Pontides, NE Turkey. *Lithos* **104**, 249–266.

BEKTAŞ, O., VAN, A. & BOYNUKALIN, S. 1987. Jurassic volcanism and its geotectonics in the eastern Pontides (NE Turkey). *Geological Bulletin of Turkey* **30**, 9–18.

BLUNDY, J.D. & HOLLAND, T.J.B. 1990. Calcic amphibole equilibria and a new amphibole-plagioclase geothermometer. *Contributions to Mineralogy and Petrology* **104**, 208–224.

BOZTUĞ, D., JONCKHEERE, R.C., WAGNER, G.A. & YEĞİNGİL, Z. 2004. Slow Senonian and fast Paleocene–Early Eocene uplift of the granitoids in the Central eastern Pontides, Turkey: apatite fission-track results. *Tectonophysics* **382**, 213–228.

BRADSHAW, T.K. & SMITH, E.I. 1994. Polygenetic Quaternary volcanism at Crater Flat, Nevada. *Journal of Volcanology and Geothermal Research* **63**, 165–182.

BUKET, E. & TEMEL, A. 1998. Major-element, trace-element, and Sr–Nd isotopic geochemistry and genesis of Varto (Muş) volcanic rocks, Eastern Turkey. *Journal of Volcanology and Geothermal Research* **85**, 405–422.

CHEN, W. & ARCULUS, R.J. 1995. Geochemical and isotopic characteristics of lower crustal xenoliths, San Francisco Volcanic Field, Arizona, U.S.A. *Lithos* **110**, 99–119.

ÇAMUR, M.Z., GÜVEN, İ.H. & ER, M. 1996. Geochemical characteristics of the eastern Pontide volcanics: an example of multiple volcanic cycles in arc evolution. *Turkish Journal of Earth Sciences* **5**, 123–144.

ÇOĞULU, E. 1975. *Petrogeologic and Geochronologic Investigation of Gümüşhane and Rize Granitic Plutons and Their Comparison*. Dissertation Thesis, İstanbul Technical University [in Turkish with English abstract, unpublished].

DENIEL, C., AYDAR, E. & GOURGAUD, A. 1998. The Hasan Dağı stratovolcano (Central Anatolia, Turkey): evolution from calc-alkaline to alkaline magmatism in a collision zone. *Journal of Volcanology and Geothermal Research* **87**, 275–302.

ELBURG, M.A., BERGEN, M.V., HOOGEWERFF, J., FODEN, J., VROON, P., ZULKARNAIN, I. & NASUTION, A. 2002. Geochemical trends across an arc-continent collision zone: magma sources and slab-wedge transfer processes below the Pantar Strait volcanoes, Indonesia. *Geochimica et Cosmochimica Acta* **66**, 2771–2789.

ELLAM, R.M. & HARMON, R.S. 1990. Oxygen isotope constraints on the crustal contributions to the subduction-related magmatism of the Aeolian Islands, Southern Italy. *Journal of Volcanology and Geothermal Research* **44**, 105–122.

EYÜBOĞLU, Y., BEKTAŞ, O. & PUL, D. 2007. Mid-Cretaceous olistostromal ophiolitic melange developed in the back-arc basin of the eastern Pontide magmatic arc, northeast Turkey. *International Geology Review* **49**, 1103–1126.

FITTON, J.G., JAMES, D. & LEEMAN, W.P. 1991. Basic magmatism associated with Late Cenozoic extension in the western United States: compositional variations in space and time. *Journal of Geophysical Research* **96**, 13693–13712.

FOLEY, S.F. & WHELLER, G.E. 1990. Parallels in the origin of the geochemical signatures of island arc volcanics and continental potassic igneous rocks: the role of residual titanites. *Chemical Geology* **85**, 1–18.

GÖRÜR, N. 1988. Timing of opening of the Black Sea basin, *Tectonophysics* **147**, 247–262.

GUO, Z., WILSON, M., LIU, J. & MAO, Q. 2006. Post-collisional, potassic and ultrapotassic magmatism of the northern Tibetan plateau: constraints on characteristics of the mantle source, geodynamic setting and uplift mechanism. *Journal of Petrology* **47**, 1177–1220.

GÜVEN, İ.H. 1993. *1:25000 Scale Geology and Compilation of the eastern Pontide*. General Directorate of Mineral Research and Exploration (MTA) of Turkey, Ankara [unpublished].

HARMS, U., CAMERON, K.L., SIMON, K. & BRATZ, H. 1997. Geochemistry and petrogenesis of metabasites from the KTB ultradeep borehole, Germany. *Geologische Rundschau* **86**, 155–166.

HAMMASTROM, J.M. & ZEN, E.A. 1986. Aluminum in hornblende: an empirical igneous geobarometer. *American Mineralogist* **71**, 1297–1313.

HAWKESWORTH, C.J., TURNER, S.P., MCDERMOTT, F., PEATE, D.W. & VAN CALSTEREN, P. 1997. U-Th isotopes in arc magmas: implications for element transfer from the subducted crust. *Science* **276**, 551–555.

HOCHSTAEDTER, A.G., GILL, J.B., TAYLOR, B., ISHIZUKA, O., YUASA, M. & MORITA, S. 2000. Across-arc geochemical trends in the Izu–Bonin arc: constraints on source composition and mantle melting. *Journal of Geophysical Research* **105**, 495–512.

HOFFMANN, A.W. 1988. Chemical differentiation of the Earth. The relationship between mantle, continental crust and oceanic crust. *Earth and Planetary Science Letters* **90**, 297–314.

HOLLISTER, L.S., GRISSOM, G.C., PETERS, E.K., STOWELL, H.H. & SISSON, V.B. 1987. Confirmation of the empirical correlation of Al in hornblende with pressure of solidification of calc-alkaline plutons. *American Mineralogist* **72**, 231–239.

IRVINE, T.N. & BARAGAR, W.R.A. 1971. A guide to the chemical classification of common volcanic rocks. *Canadian Journal of Earth Sciences* **8**, 523–548.

JICA 1986. *The Republic of Turkey Report on the Cooperative Mineral Exploration of Gümüşhane Area, Consolidated Report*. Japanese International Cooperation Agency, Metal Mining Agency of Japan.

KAYGUSUZ, A. 2000. *Petrographic and Geochemical Investigations of rock Outcrops of Torul and Nearby Area*. PhD Thesis, Karadeniz Technical University, Trabzon [in Turkish with English abstract, unpublished].

KAYGUSUZ, A. 2009. K/Ar ages and geochemistry of the collision related volcanic rocks in the Ilıca (Erzurum) area, eastern Turkey. *Neues Jahrbuch für Mineralogie* **186**, 21–36.

KAYGUSUZ, A. & AYDINÇAKIR, E. 2009. Mineralogy, whole-rock and Sr-Nd isotope geochemistry of mafic microgranular enclaves in Cretaceous Dağbaşı granitoids, eastern Pontides, NE Turkey: evidence of magma mixing, mingling, and chemical equilibration. *Chemie der Erde Geochemistry* **69**, 247–277.

KAYGUSUZ, A., CHEN, B., ASLAN, Z., SIEBEL, W. & ŞEN, C. 2009. U-Pb zircon SHRIMP ages, geochemical and Sr-Nd isotopic compositions of the Early Cretaceous I-type Sarıosman pluton, eastern Pontides, NE Turkey. *Turkish Journal of Earth Sciences* **18**, 549–581.

KAYGUSUZ, A. & ŞEN, C. 2010. Calc-alkaline I-type plutons in the eastern Pontides, NE Turkey: U-Pb zircon ages, geochemical and Sr-Nd isotopic compositions. *Chemie der Erde Geochemistry*. DOI:10.1016/j.chemer.2010.07.005.

KAYGUSUZ, A., ŞEN, C. & ASLAN, Z. 2006. Petrographic and petrological features of Torul (Gümüşhane) volcanites (NE Turkey); evidences for fractional crystallisation and magma mixing/mingling. *Geological Bulletin of Turkey* **49**, 49–82.

KAYGUSUZ, A., WOLFGANG, S., ŞEN, C. & SATIR, M. 2008. Petrochemistry and petrology of I-type granitoids in an arc setting: the composite Torul pluton, eastern Pontides, NE Turkey. *International Journal of Earth Sciences* **97**, 739–764.

KAZMIN, V.G., SBORTSHIKOV, I.M., RICOU, L.E., ZONENSHAIN, L.P., BOULIN, J. & KNIPPER, A.L. 1986. Volcanic belts as marker of the Mesozoic–Cenozoic evolution of Tethys. *Tectonophysics* **123**, 123–152.

KESKİN, M., PEARCE, J.A., KEMPTON, P.D. & GREENWOOD, P. 2006. Magma-crust interactions and magma plumbing in a post-collisional setting: geochemical evidence from the Erzurum-Kars volcanic plateau, eastern Turkey. *In*: DILEK, Y. & PAVLIDES, S. (eds), *Postcollisional Tectonics and Magmatism in the Mediterranean Region and Asia*. Geological Society of America Special Paper **409**, 475–505.

KORKMAZ, S., TÜYSÜZ, N., ER, M., MUSAOĞLU, A. & KESKİN, İ. 1995. Stratigraphy of the eastern Pontides, NE Turkey. *In*: ERLER, A., ERCAN, T., BİNGÖL, E. & ÖRÇEN, S. (eds), *Geology of the Black Sea Region*. General Directorate of Mineral Research and Exploration (MTA), and Chamber of Geological Engineers, Ankara, 59–69.

KURT, H., ASAN, K. & RUFFET, G. 2008. The relationship between collision-related calc-alkaline, and within-plate alkaline volcanism in the Karacadağ area (Konya-Türkiye, central Anatolia). *Chemie der Erde* **68**, 155–176.

LAMBERT, R.J. & HOLLAND, J.G. 1974. Yttrium geochemistry applied to petrogenesis utilizing calcium–yttrium relationships in minerals and rocks. *Geochimica et Cosmochimica Acta* **38**, 1393–1414.

LE MAITRE, R.W., STRECKEISEN, A., ZANETTIN, B., LE BAS, M.J., BONIN, B., BATEMAN, P., BELLIENI, G., DUDEK, A., EFREMOVA, S., KELLER, J., LAMERE, J., SABINE, P.A., SCHMID, R., SORENSEN, H. & WOOLLEY, A.R. 2002. *Igneous Rocks: A Classification and Glossary of Terms, Recommendations of the International Union of Geological Sciences, Subcommission of the Systematics of Igneous Rocks.* Cambridge University Press, Cambridge, U.K. London, Special Publications **16**, 59–76.

LEAKE, B.E., WOOLEY, A.R., ARPS, C.E.S., BIRCH, W.D., GILBERT, M.C., GRICE, J.D., HAWTHORNE, F.C., KATO, A., KISCH, H.J., KRIVOVICHEV, V.G., LINTHOUT, K., LAIRD, J., MANDARINO, J., MARESCH, W.V., NICKHEL, E.H., ROCK, N.M.S., SCHUMACHER, J.C., SMITH, D.C., STEPHENSON, N.C.N., UNGARETTI, L., WHITTAKER, E.J.W. & YOUZHI, G. 1997. Nomenclature of amphiboles report of the subcommittee on amphiboles of the International Mineralogical Association Commission on New Minerals and Mineral Names. *European Journal of Mineralogy* **9**, 623–651.

LIEW, T.C. & HOFFMAN, A.W. 1988. Precambrian crustal components, plutonic associations, plate environment of the Hercynian fold Belt of Central Europe: indications from a Nd and Sr isotopic study. *Contributions to Mineralogy and Petrology* **98**, 129–138.

MADEN, N., GELİŞLİ, K., EYÜBOĞLU, Y. & BEKTAŞ, O. 2009. Determination of tectonic and crustal structure of the eastern Pontide orogenic belt (NE Turkey) using gravity and magnetic data. *Pure and Applied Geophysics* **166**, 1987–2006.

MCDERMOTT, F., DELFIN, F.G., DEFANT, M.J., TURNER, S. & MAURY, R. 2005. The petrogenesis of magmas from Mt. Bulusan and Mayon in the Bicol arc, the Philippines. *Contributions to Mineralogy and Petrology* **150**, 652–670.

MORIMOTO, M. 1988. Nomenclature of pyroxenes. *Mineralogical Magazine* **52**, 535–550.

OKAY, A.İ. & ŞAHİNTÜRK, Ö. 1997. Geology of the eastern Pontides. *In*: ROBINSON, A.G. (ed), *Regional and Petroleum Geology of the Black Sea and Surrounding Region.* American Association of Petroleum Geologists (AAPG) Memoir **68**, 291–311.

ÖZSAYAR, T., PELİN, S. & GEDİKOĞLU, A. 1981. Cretaceous in the eastern Pontides. *Karadeniz Technical University, Journal of Earth Sciences* **1**, 65–14 [in Turkish with English abstract].

PEARCE, J.A. 1982. Trace element characteristics of lavas from destructive plate boundaries. *In*: THORPE, R.S. (ed), *Andesites: Orogenic Andesites and Related Rocks.* John Wiley, London, 525–548.

PEARCE, J.A. 1983. Role of the sub-continental lithosphere in magma genesis at active continental margins. *In*: HAWKESWORTH, C.J. & NORRY, M.J. (eds), *Continental Basalts and Mantle Xenoliths.* Shiva, Cheshire, 230–249.

PEARCE, J.A., BENDER, J.F., DE LONG, S.E., KIDD, W.S.F., LOW, P.J., GÜNER, Y., SAROĞLU, F., YILMAZ, Y., MOORBATH, S. & MITCHELL, J.J. 1990. Genesis of collision volcanism in eastern Anatolia Turkey. *Journal of Volcanology and Geothermal Research* **44**, 189–229.

PEARCE, J.A. & PARKINSON, I.J. 1993. Trace element models for mantle melting: application to volcanic arc petrogenesis. *In*: PRICHARD, H.M., ALABASTER, T., HARRISI, N.B.W. & NEARY, C.R. (eds), *Magmatic Processes and Plate Tectonics.* Geological Society, London, Special Publications **76**, 373–403.

PEARCE, J.A. & PEATE, D.W. 1995. Tectonic implications of the composition of volcanic arc magmas. *Annual Review of Earth and Planetary Science Letters* **23**, 251–285.

PECCERILLO, R. & TAYLOR, S.R. 1976. Geochemistry of Eocene calc-alkaline volcanic rocks from the Kastamonu area, northern Turkey. *Contributions to Mineralogy and Petrology* **58**, 63–81.

QIAO, G. 1988. Normalization of isotopic dilution analyses–a new program for isotope mass spectrometric analysis. *Scientia Sinica* **31**, 1263-1268.

ROBINSON, A.G., BANKS, C.J., RUTHERFORD, M.M. & HIRST, J.P.P. 1995. Stratigraphic and structural development of the eastern Pontides, Turkey. *Journal of the Geological Society*, London **152**, 861–872.

SAUNDERS, A.D. & TARNEY, J. 1984. Geochemical characteristics of basaltic volcanism within back-arc basins. *In*: KOKELAAR, B.P. & HOWELLS, M.F. (eds), *Marginal Basin Geology.* Geological Society, London, Special Publications **16**, 59–76.

SCHMIDBERGER, S.S. & HEGNER, E. 1999. Geochemistry and isotope systematics of calc-alkaline volcanic rocks from the Saar-Nahe basin (SW Germany) – implications for Late Variscan orogenic development. *Contributions to Mineralogy and Petrology* **135**, 373–385.

ŞEN, C. 2007. Jurassic volcanism in the eastern Pontides: is it rift related or subduction related? *Turkish Journal of Earth Sciences* **16**, 523–539.

ŞEN, C., ARSLAN, M. & VAN, A. 1998. Geochemical and petrological characteristics of the Pontide Eocene (?) alkaline province, NE Turkey. *Turkish Journal of Earth Sciences* **7**, 231–239.

ŞEN, P.A., TEMEL, A. & GOURGA, A. 2004. Petrogenetic modelling of Quaternary post-collisional volcanism: a case study of central and eastern Anatolia. *Geological Magazine* **141**, 81–98.

ŞENGÖR, A.M.C. & YILMAZ, Y. 1981. Tethyan evolution of Turkey: a plate tectonic approach. *Tectonophysics* **75**, 181–241.

ŞENGÖR, A.M.C., ÖZEREN, S., GENÇ, T. & ZOR, E. 2003. East Anatolian high plateau as a mantle-supported, north–south shortened domal structure. *Geophysical Research Letter* 30 (24), 8045. doi:10.1029/2003GL017858.

SMITH, E.I., SANCHEZ, A., WALKER, J.D. & WANG, K. 1999. Geochemistry of mafic magmas in the Hurricane Volcanic field, Utah: implications for small- and large-scale chemical variability of the lithospheric mantle. *Journal of Geology* **107**, 433–448.

SUN, S.S. & MCDONOUGH, W.F. 1989. Chemical and isotopic systematics of oceanic basalts: implications for mantle composition and processes. *In*: SAUNDERS, A.D. & NORRY, M.J. (eds), *Magmatism in the Ocean Basins*. Geological Society, London, Special Publications **42**, 313–345.

TAYLOR, S.R. & MCLENNAN, S.M. 1985. *The Continental Crust: Its Composition and Evolution*. Blackwell, Scientific Publication, Oxford.

TEMEL, A., GÜNDOĞDU, M.N., GOURGAUD, A. & LE PENNEC, J.L. 1998. Ignimbrites of Cappadocia (Central Anatolia, Turkey): petrology and geochemistry. *Journal of Volcanology and Geothermal Research* **85**, 447–471.

TEMİZEL, İ. 2008. *Petrography, Petrochemistry, ^{40}Ar-^{39}Ar Geochemistry, Sr-Nd Isotope Geochemistry and Petrogenesis of the Ulubey (Ordu-NE Turkey) Area Tertiary volcanics*. PhD Thesis, Karadeniz Technical University, Trabzon [in Turkish with English abstract, unpublished].

TEMİZEL, İ. & ARSLAN, M. 2003. Geochemical modelling of magmatic processes in the evolution of Tertiary volcanics in the İkizce (Ünye-Ordu) area, NE-Turkey. *Süleyman Demirel University, Journal of Science Institute* **7**, 161–177 [in Turkish with English abstract].

TEMİZEL, İ. & ARSLAN, M. 2005. Mineral chemistry and petrochemistry of Tertiary calc-alkaline volcanic rocks in the İkizce (Ordu) area, NE Turkey. *Earth Sciences* **26**, 25–47 [in Turkish with English abstract].

TEMİZEL, İ. & ARSLAN, M. 2008. Petrology and geochemistry of Tertiary volcanic rocks from the İkizce (Ordu) area, NE Turkey: implications for the evolution of the eastern Pontide paleomagmatic arc. *Journal of Asian Earth Sciences* **31**, 439–463.

TEMİZEL, İ. & ARSLAN, M. 2009. Mineral chemistry and petrochemistry of post-collisional Tertiary mafic to felsic cogenetic volcanics in the Ulubey (Ordu) area, eastern Pontides, NE Turkey. *Turkish Journal of Earth Sciences* **18**, 29–53.

THIRLWALL, M.F., GRAHAM, A.M., ARCULUS, R.J., HARMON, R.S. & MACPHERSON, C.G. 1996. Resolution of the effects of crustal assimilation, sediment subduction, and fluid transport in island arc magmas: Pb-Sr-Nd-O isotope geochemistry of Grenada, Lesser Antilles. *Geochimica et Cosmochimica Acta* **60**, 4785–4810.

THOMPSON, R.N., MORRISON, M.A., HENDRY, G.L. & PARRY, S.J. 1984. An assessment of the relative roles of crust and mantle in magma genesis: an elemental approach. *Philosophical Transactions of the Royal Society, London* **A310**, 549–590.

TOKEL, S. 1977. Eocene calc-alkaline andesites and geotectonism in Black Sea Region. *Geological Society of Turkey Bulletin* **20**, 49–54 [in Turkish with English abstract].

TOPUZ, G. 2002. Retrograde P-T path of anatectic migmatites from the Pulur Massif, eastern Pontides, NE Turkey: petrological and microtextural constraints. 1st International *Symposium of the Faculty of Mines (İTÜ) on Earth Sciences and Engineering Abstracts, İstanbul, Turkey*, p. 110.

TOPUZ, G., ALTHERR, R., SATIR, M. & SCHWARZ, W. 2001. Age and metamorphic conditions of low-grade metamorphism in the Pulur Massif, NE Turkey. *Fourth International Turkish Geology Symposium Abstracts, Adana, Turkey*, p. 215.

VAROL, E., TEMEL, A., GOURGAUD, A. & BELLON, H. 2007. Early Miocene 'adakite-like' volcanism in the Balkuyumcu region, central Anatolia, Turkey: petrology and geochemistry. *Journal of Asian Earth Sciences* **30**, 613–628.

WEAVER, B.L., WOOD, D.A., TARNEY, J. & JORON, J. 1987. Geochemistry of ocean island basalt from the South Atlantic: Ascension, Bouvet, St. Helena, Gough and Tristan da Cunda. *In*: FITTON, J.G. & UPTON, B.G.J. (eds), *Alkaline Igneous Rocks*. Geological Society, London, Special Publications **30**, 253–267.

WHITE, W.M. & PATCHETT, J. 1984. Hf–Nd–Sr isotopes and incompatible element abundances in island arcs: implications for magma origins and crust-mantle evolution. *Earth and Planetary Science Letters* **67**, 167–185.

WILSON, M., TANKUT, A. & GÜLEÇ, N. 1997. Tertiary volcanism of the Galatia province, north-west Central Anatolia, Turkey. *Lithos* **42**, 105–121.

YALÇIN, H., GÜNDOĞDU, M.N., GOURGAUD, A., VIDAL, P. & UÇURUM, A. 1998. Geochemical characteristics of Yamadağı volcanics in central east Anatolia: an example from collision-zone volcanism. *Journal of Volcanology and Geothermal Research* **85**, 303–326.

YILMAZ, C. & KORKMAZ S. 1999. Basin development in the eastern Pontides, Jurassic to Cretaceous, NE Turkey. *Zentralblatt für Geologie und Paläontologie, Teil I* **10–12**, 1485–1494.

YILMAZ, Y. 1972. *Petrology and Structure of the Gümüşhane Granite and Surrounding Rocks, North-eastern Anatolia*. PhD Thesis, University of London [unpublished].

YILMAZ, Y., TÜYSÜZ, O., YİĞİTBAŞ, E., GENÇ, Ş.C. & ŞENGÖR, A.M.C. 1997. Geology and tectonics of the Pontides. *In*: ROBINSON, A.G. (ed), *Regional and Petroleum Geology of the Black Sea and Surrounding Region*. American Association of Petroleum Geologists (AAPG) Memoir **68**, 183–226.

YÜCEL, C., ARSLAN, M., TEMİZEL, İ. & ABDİOĞLU, E. 2009. Mineralogical-petrographical and volcanic facies characteristics of the Tertiary volcanic rocks between Trabzon and Giresun areas, eastern Pontide northern zone, Turkey. *2nd International Symposium on the Geology of the Black Sea Region Abstract Book*, p. 236.

ZELLMER, G.F., ANNEN, C., CHARLIER, B.L.A., GEORGE, R.M.M., TURNER, S.P. & HAWKESWORTH, C.J. 2005. Magma evolution and ascent at volcanic arcs: constraining petrogenetic processes through rates and chronologies. *Journal of Volcanology and Geothermal Research* **140**, 171–191.

ZHANG, H.-F., SUN, M., ZHOU, X. H., FAN, W.M. & YIN, J.F. 2002. Mesozoic lithosphere destruction beneath the north China Craton: evidence from major, trace element, and Sr-Nd-Pb isotope studies of Fangcheng Basalts. *Contributions to Mineralogy and Petrology* **144**, 241–253.